Diffusion Onsager Coefficients L_{ij} for the NaCl + Na_2SO_4 + H_2O System at 298.15 K[†]

Joseph A. Rard*

4363 Claremont Way, Livermore, California 94550

John G. Albright[‡]

Department of Chemistry, Texas Christian University, Ft. Worth, Texas 76129

Donald G. Miller[§]

2862 Waverly Way, Livermore, California 94551

The isothermal diffusion Onsager coefficients L_{ij} have been calculated and the Onsager reciprocal relation (ORR) has been tested for 23 compositions of the NaCl + Na_2SO_4 + H_2O system at 298.15 K. The calculations are based on our previously reported extensive set of Fick's law based diffusion coefficients measured using the high-quality Gosting diffusiometer and volumetric measurements made with a vibrating-tube densimeter or (at a few compositions) with pycnometry. These calculations also require the four chemical-potential concentration derivatives, which were obtained by reanalysis of available isopiestic data using a hybrid thermodynamic model. This model uses an extended form of Pitzer's ion-interaction model to represent the single-salt thermodynamic activities but uses the mixing terms from Scatchard's neutral-electrolyte model. Because of the ORR, the two cross-term diffusion Onsager coefficients should be equal, i.e., $L_{12} = L_{21}$, on either the solvent-fixed or volume-fixed reference frames. The ORR was actually tested using the experimental volume-fixed diffusion coefficients, with an equation that reduces the propagation-of-errors calculations by removing unnecessary terms. The ORR is found to be satisfied for 22 of the 23 compositions when estimated errors (usually 5 to 10 % for the chemical-potential derivatives, depending on the composition, 4 times the standard errors for diffusion coefficients or scatter observed from cross-plots, whichever is larger) are assigned for the input quantities.

Introduction

Diffusion of a solute i in a binary solution without bulk solution flow can be described by Fick's second law (formulated in 1855)[1] for non-steady-state diffusion

$$(J_i)_R = -(D_i)_R \nabla C_i \quad (1)$$

where $(J_i)_R$ is the diffusional flow, $(D_i)_R$ is the binary-solution diffusion coefficient, C_i is the molar concentration of this solute, and the subscript R refers to an arbitrary reference frame. Onsager and Fuoss,[2] for the solvent-fixed reference frame, and Onsager[3] proposed that Fick's second law be extended to an n-component system in the form of

$$(J_i)_R = -\sum_{j=1}^{n-1} (D_{ij})_R \nabla C_j \quad (2)$$

where the flow of component i not only depends on its own concentration gradient but also is coupled to the concentration gradients of the other solutes. The summation is not over all n components because the diffusion coefficient of the component chosen to be the solvent is not independent of those of the solutes, which is a consequence of the choice of a reference frame.[4,5] The $(D_{ii})_R$ are called main-term diffusion coefficients, the $(D_{ij})_R$ ($i \neq j$) are called cross-term diffusion coefficients, and their numerical values depend on the reference frame R.

Reference frames are important in describing diffusion, and equations are available for transforming quantities from one frame into those of another.[4,5] We report results in both the volume-fixed and solvent-fixed frames.

Most experimental measurements are done in the volume-fixed reference frame, which is the case when the concentration differences are small and the diffusion cell is closed at one end. For this reference frame, the diffusion coefficient matrix of eq 2 has real, positive eigenvalues and its determinant is positive. These are the criteria required for stable diffusion boundaries (see original references cited in ref 4). When necessary, the volume-fixed flows, diffusion coefficients, and diffusion Onsager coefficients will have the subscript V.

The solvent-fixed reference frame gives a simpler representation in the linear irreversible thermodynamics description of diffusion and is the best for the theoretical description of electrolyte systems. When necessary, the solvent-fixed flows, diffusion coefficients, and diffusion Onsager coefficients will have the subscript 0.

In the following discussion, we will emphasize ternary solutions of two electrolytes with a common ion in a neutral solvent (in this case H_2O) and will denote the two solutes as

[†] Part of the special issue "Robin H. Stokes Festschrift".

* To whom correspondence should be addressed. E-mail: solution_chemistry2@comcast.net.
[‡] E-mail: j.albright@tcu.edu.
[§] E-mail: don.miller9@comcast.net.

10.1021/je800725k CCC: $40.75
Published on Web 12/29/2008

components 1 and 2 and the solvent as component 0. (Note that if the two electrolytes do not share a common ion, then they form a quaternary system for diffusion and therefore have nine diffusion coefficients.)

The above equations were written for the general case of three-dimensional diffusion, but in most accurate diffusion measurements, the flow is restricted to one direction, so that ∇ can be replaced by $\partial/\partial x$ where x is a Cartesian coordinate. The most common experimental situation in diffusion measurements involves gravitational stability achieved by layering of a less dense and generally less concentrated solution over a denser and generally more concentrated one. For this case, diffusive flows usually but not always move upward from higher to lower concentrations. As noted above, the typically small concentration differences used in the diffusion experiments yield diffusion coefficients and flows in the volume-fixed reference frame. Equation 2 then takes the specific form

$$(J_i)_V = -\sum_{j=1}^{n-1} (D_{ij})_V \left(\frac{\partial C_j}{\partial x}\right) \tag{3}$$

and for a three-component system

$$(J_1)_V = -(D_{11})_V \left(\frac{\partial C_1}{\partial x}\right) - (D_{12})_V \left(\frac{\partial C_2}{\partial x}\right) \tag{4a}$$

$$(J_2)_V = -(D_{21})_V \left(\frac{\partial C_1}{\partial x}\right) - (D_{22})_V \left(\frac{\partial C_2}{\partial x}\right) \tag{4b}$$

A fundamental analysis of diffusive transport, based on irreversible thermodynamics,[4] indicates that the driving forces for diffusion are not the concentration gradients, as assumed in Fick's phenomenological laws, but rather the gradients of the partial molar Gibbs energy (chemical potential), $(\partial G_j/\partial x)$.[4−9] The simplest representation of diffusion based on these chemical-potential gradients is in terms of solvent-fixed flows and diffusion Onsager coefficients.[4] On the solvent-fixed frame,

$$(J_i)_0 = -\sum_{j=1}^{n-1} (L_{ij})_0 \left(\frac{\partial G_j}{\partial x}\right)_{p,T} \tag{5}$$

where G_j is the partial molar Gibbs energy (chemical potential) of solute component j in the mixture (sometimes denoted as μ_j, especially in the older literature), $(J_i)_0$ is the solvent-fixed flow, and $(L_{ij})_0$ is called a thermodynamic diffusion coefficient or diffusion Onsager coefficient. When eq 2 is written in terms of solvent-fixed flows and diffusion coefficients and compared with eq 5, then

$$(D_{ij})_0 = \sum_{k=1}^{n-1} (L_{ik})_0 \mu_{ij} \tag{6}$$

where for brevity, and in common with the published literature, we denote *molarity* chemical-potential derivatives as

$$\mu_{ij} = \left(\frac{\partial G_i}{\partial C_j}\right)_{p,T} = \left(\frac{\partial \mu_i}{\partial C_j}\right)_{p,T} \tag{7}$$

For a three-component system, there are four such derivatives for the solutes, μ_{11}, μ_{12}, μ_{21}, and μ_{22}, where in general $\mu_{12} \neq \mu_{21}$.[10]

$(L_{ij})_0$ are obtained from the solution of eq 6 (four such equations for ternary systems)[10] or by matrix inversion.

The partial molar Gibbs energy of a solute is related to the logarithm of its activity coefficient, and accurate activity coefficient models for mixtures are usually based on the *molality* composition scale rather than the *molarity*. Thus, the derivatives needed for eq 6 are generally evaluated with respect to the solute molalities and then multiplied by the appropriate derivatives of the molality with respect to the molarity (see below for the equations).

Experimental cross-term diffusion coefficients are, in general, not equal and can be large, as found, for example, for D_{12} in the NaCl + $MgCl_2$ + H_2O system at 298.15 K for certain solute ratios.[11] These cross-term coefficients may even have opposite signs, as is observed, for example, at certain compositions of the KCl + $ZnCl_2$ + H_2O system at 298.15 K.[12] However, when the diffusion Onsager coefficients are expressed in the proper reference frame, then their cross-term coefficients should obey the Onsager reciprocal relation (ORR). For the solvent-fixed flows expressed by eq 5, the ORR is

$$(L_{12})_0 = (L_{21})_0 \tag{8a}$$

The experimental diffusion coefficients on the volume-fixed reference frame, $(D_{ij})_V$, lead to a type of diffusion Onsager coefficient on the volume-fixed reference frame, but they do not obey the ORR when the driving force is defined as in eq 5. However, by transformation of the driving force to be consistent with the invariance of entropy production,[4,10] the resulting volume-fixed $(L_{ij})_V$ do obey the ORR,[4,14]

$$(L_{12})_V = (L_{21})_V \tag{8b}$$

although relationships between $(D_{ij})_V$ and $(L_{ij})_V$ are more complicated than those given by eq 6.[10] (See the Appendix.)

Numerous tests have been made of the ORR relation based on eq 8b for aqueous electrolyte and electrolyte + nonelectrolyte mixtures.[10,13−15] The ORR has generally been found to be obeyed within realistic uncertainty limits. However, the uncertainties for these tests can be fairly large mainly because the chemical-potential concentration derivatives μ_{ij} calculated from eq 7 can have large uncertainties. In the past, on the basis of examination of the chemical-potential derivatives calculated from different fits of comparable quality to a ternary-solution activity data set, we have found that the errors in the chemical-potential derivatives are commonly about 5 to 10 % of their values. The error estimates for the present system will be discussed below.

Uncertainties in the diffusion coefficients can also make significant contributions to uncertainties in the $(L_{ij})_0$ and $(L_{ij})_V$ values. Diffusion coefficients $(D_{ij})_V$ measured with the Gosting diffusiometer,[16] the world's finest optical interferometer for diffusion measurements, were previously assigned uncertainties described by an earlier "rule-of-thumb" as roughly 4 times the statistical errors calculated by the propagation-of-errors method,[11] and those measured with other methods or other diffusiometers will likely have even larger uncertainties. This rule of thumb was based on earlier work with 10 to 12 diffusion patterns recorded on glass photographic plates. A much greater amount of data per experiment is collected with this now automated diffusiometer, as described in the next paragraph, and the uncertainties will be discussed below.

The NaCl + Na_2SO_4 + H_2O system at 298.15 K has the potential of giving the most accurate tests of the ORR. We have reported an extensive series of diffusion coefficient measurements for this system[17−21] using the Gosting diffusiometer after it had been moved to its present location at Texas Christian University. Two compositions were studied with Gouy interferometry with the diffusion patterns recorded on glass photographic plates. The other 21 compositions were studied with Rayleigh interferometry after data collection was automated with a computer-controlled scanner using a 6 cm linear diode array.

Table 1. Values of the Experimental Volume-Fixed Diffusion Coefficients $(D_{ij})_V$ at $T = 298.15$ K at Each of the Mean Concentrations Used in the Diffusion Studies[a]

z_1	$\langle\bar{C}_1\rangle$ /mol·dm^{-3}	$\langle\bar{C}_2\rangle$ /mol·dm^{-3}	$10^9(D_{11})_V$/m^2·s^{-1}	$10^9(D_{12})_V$/m^2·s^{-1}	$10^9(D_{21})_V$/m^2·s^{-1}	$10^9(D_{22})_V$/m^2·s^{-1}
			$\langle\bar{C}_T\rangle = 0.5$ mol·dm^{-3}			
1	0.49998	0	1.4747 ± 0.001	0.166 ± 0.015	0	0.906 ± 0.015
0.95	0.47493	0.02499 (**1**)[b]	1.5018 ± 0.0005	0.1723 ± 0.0011	−0.0190 ± 0.0002	0.8873 ± 0.0004
0.90	0.45002	0.05000 (**2**)	1.5317_5 ± 0.0011	0.1874 ± 0.0018	-0.0398_5 ± 0.0004	0.8713 ± 0.0007
0.75	0.37499	0.12500 (**3**)	1.5785 ± 0.0011	0.1653 ± 0.0017	−0.0802 ± 0.0004	0.8473 ± 0.0007
0.50	0.25002	0.24998 (**4**)	1.6250 ± 0.0073	0.1390 ± 0.0086	−0.1312 ± 0.0027	0.8125 ± 0.0032
0.25	0.12499	0.37501_5 (**5**)	1.6591 ± 0.0072	0.0698 ± 0.0083	−0.1705 ± 0.0027	0.7997 ± 0.0031
0	0	0.50000	1.681 ± 0.002	0	−0.195 ± 0.006	0.7932 ± 0.001
0	0	0.50000	1.681 ± 0.002	0	−0.195 ± 0.006	0.7937 ± 0.001
			$\langle\bar{C}_T\rangle = 1.0$ mol·dm^{-3}			
1	1.00138	0	1.4822 ± 0.001	0.197 ± 0.015	0	0.858 ± 0.015
0.95	0.94960	0.04997 (**6**)	1.4873 ± 0.0004	0.2114 ± 0.0006	$-0.0148 \pm 0.0001_5$	0.8302 ± 0.0002
0.90	0.90025_5	0.09999_5 (**7**)	1.5117 ± 0.0005	0.2324 ± 0.0008	−0.0349 ± 0.0002	0.8032 ± 0.0003
0.75	0.74990	0.24940 (**8**)	1.5373 ± 0.0034	0.2372 ± 0.0051	−0.0758 ± 0.0014	0.7486 ± 0.0020
0.50	0.49999	0.49996 (**9**)	1.5259 ± 0.0005	0.1922 ± 0.0007	−0.1158 ± 0.0002	0.6911 ± 0.0003
0.25	0.25000	0.74998 (**10**)	1.4726 ± 0.0011	0.1107 ± 0.0016	−0.1305 ± 0.0005	0.6616 ± 0.0006
0	0	0.99999	1.421 ± 0.027	0	−0.131 ± 0.021	0.6545 ± 0.001
0	0	1.00002	1.421 ± 0.027	0	−0.131 ± 0.021	0.6546 ± 0.001
			$\langle\bar{C}_T\rangle = 1.5$ mol·dm^{-3}			
1	1.50002	0	1.4978 ± 0.001	0.277 ± 0.015	0	0.808 ± 0.015
0.95	1.42493_5	0.07498 (**11**)	1.5037 ± 0.0008	0.2882_5 ± 0.0013	−0.0170 ± 0.0003	0.7759_5 ± 0.0005
0.90	1.34911	0.14990 (**12**)	1.5018 ± 0.0007	0.2970 ± 0.0011	−0.0305 ± 0.0003	0.7444 ± 0.0004
0.75	1.12447	0.37497 (**13**)	1.4964 ± 0.0012	0.3039 ± 0.0017	−0.0655 ± 0.0005	0.6737 ± 0.0007
0.50	0.74995	0.74996 (**14**)	1.4278 ± 0.0012	0.2603 ± 0.0017	−0.0917 ± 0.0005	0.5993 ± 0.0006
0.25	0.37505	1.12516 (**15**)	1.2953 ± 0.0008	0.1372 ± 0.0011	−0.0809 ± 0.0003	0.5738 ± 0.0004
0	0	1.50007	1.145 ± 0.02	0	−0.03 ± 0.02	0.5712 ± 0.001
0	0	1.50001	1.145 ± 0.02	0	−0.03 ± 0.02	0.5706 ± 0.001
			$\langle\bar{C}_T\rangle = 2.0$ mol·dm^{-3}			
1	1.99994	0	1.5182 ± 0.001	0.338	0	0.763 ± 0.015
0.95	1.89909	0.09994 (**16**)	1.5021 ± 0.0013	0.3676 ± 0.0020	−0.0122 ± 0.0005	0.7256 ± 0.0007
0.90	1.80007	0.19998 (**17**)	1.4973 ± 0.0011	0.3976 ± 0.0016	−0.0259 ± 0.0005	0.6878 ± 0.0006
			$\langle\bar{C}_T\rangle = 3.0$ mol·dm^{-3}			
1	3.00019	0	1.5586 ± 0.001	0.591	0	0.666 ± 0.015
0.95	2.84561	0.14976 (**18**)	1.5280 ± 0.0005	0.5999 ± 0.0008	−0.0087 ± 0.0002	$0.6275 \pm 0.0002_5$
0.90	2.70025	0.30004 (**19**)	1.5005 ± 0.0007	0.6089 ± 0.0013	−0.0160 ± 0.0003	0.5889 ± 0.0003
			$\langle\bar{C}_T\rangle = 4.0$ mol·dm^{-3}			
1	4.00017_5	0	1.5868 ± 0.001	0.866	0	0.572 ± 0.015
0.95	3.78944_5	0.19943 (**20**)	1.5370_5 ± 0.0007	$0.8299 \pm 0.0016_5$	-0.0026_5 ± 0.0003	0.5407 ± 0.0003
0.90	3.60091_5	0.40010 (**21**)	1.4770 ± 0.0012	0.7938 ± 0.0017	−0.0005 ± 0.0005	0.5099 ± 0.0005
			$\langle\bar{C}_T\rangle = 5.0$ mol·dm^{-3}			
1	4.99938	0	1.5834 ± 0.001	1.019	0	0.500 ± 0.015
0.95	4.72944	0.24890 (**22**)	1.5086 ± 0.0007	0.9941 ± 0.0009	0.0048 ± 0.0003	0.4686 ± 0.0003
0.90	4.50638	0.50070 (**23**)	1.4218 ± 0.0007	0.9691 ± 0.0025	0.0126 ± 0.0003	0.4370 ± 0.0003

[a] The values of $(D_{ij})_V$ of the mixtures and their standard errors (from propagation-of-errors calculations) were taken from refs 17 to 21. For the limiting case as $z_1 \rightarrow 1$, $(D_{11})_V = D_V$ of NaCl(aq) at the same molar concentration, $(D_{21})_V = 0$, $(D_{12})_V$ is an extrapolated value and $(D_{22})_V$ is an extrapolated value equal to the trace diffusion coefficient of SO_4^{2-} in NaCl(aq). Similarly, for the limiting case as $z_1 \rightarrow 0$, $(D_{22})_V = D_V$ of Na_2SO_4(aq) at the same molar concentration, $(D_{12})_V = 0$, $(D_{21})_V$ is an extrapolated value and $(D_{11})_V$ is an extrapolated value equal to the trace diffusion coefficient of the Cl^- ion in Na_2SO_4(aq). [b] The numbers given in boldface font are numerical designators that are used in the subsequent tables.

This automated data acquisition yields improved precision in the diffusion coefficients because of the considerably larger amount of data that is acquired during each experiment, equivalent to photographic diffusion patterns taken at 50 different times and at more fringe positions for each time. We earlier reported extensive diffusion measurements for the limiting binary solutions NaCl + H_2O and Na_2SO_4 + H_2O at 298.15 K with a fractional uncertainty of about ± 0.1 to 0.2 % using a different diffusiometer at Lawrence Livermore National Laboratory.[22,23] However, during the course of the mixture studies,[17−21] we made additional measurements (seven for NaCl and nine for Na_2SO_4) for the binary solutions with a greater fractional precision (reproducibility) of ± 0.06 %.

Extensive density data were also reported for the same NaCl + Na_2SO_4 + H_2O mixtures,[17−21] which allowed us to calculate the partial molar volumes $\bar{V}_i$ of each component. These $\bar{V}_i$ values, in turn, were used with the experimental $(D_{ij})_V$ to derive the corresponding solvent-fixed $(D_{ij})_0$ values.

The diffusion coefficients and densities of the NaCl + Na_2SO_4 + H_2O mixtures[17−21] were measured at total mean concentrations of $\langle\bar{C}_T\rangle = \langle\bar{C}_1\rangle + \langle\bar{C}_2\rangle$ = (0.500, 1.000, and 1.500) mol·dm^{-3} at NaCl molarity fractions of z_1 = {1 (binary NaCl solutions), 0.95, 0.90, 0.75, 0.50, 0.25, and 0 (binary Na_2SO_4 solutions)}, along with measurements at $\langle\bar{C}_T\rangle = \langle\bar{C}_1\rangle + \langle\bar{C}_2\rangle$ = (2.0, 3.0, 4.0, and 5.0) mol·dm^{-3} at NaCl molarity fractions of z_1 = 1, 0.95, and 0.90 (the higher concentration measurements[20,21] could not be extended over the full range of z_1 because of Na_2SO_4 solubility limitations). These diffusion coefficients at each constant $\langle\bar{C}_T\rangle$ were graphically extrapolated to $z_1 = 1$ to yield the limiting value of $(D_{12})_V$ and of $(D_{22})_V$ (the sulfate trace diffusion coefficient in a NaCl solution) and correspondingly extrapolated to $z_1 = 0$ to yield the limiting value of $(D_{21})_V$ and of $(D_{11})_V$ (the chloride trace diffusion coefficient in a Na_2SO_4 solution). Because we have determined the values of $(D_{ij})_V$ and $(D_{ij})_0$ as functions of both $\langle\bar{C}_T\rangle$ and z_1, we can use cross plotting

Table 2. Values of the Derived Solvent-Fixed Diffusion Coefficients $(D_{ij})_0$ at $T = 298.15$ K at Each of the Mean Concentrations Used in the Diffusion Studies[a]

z_1	$\langle\bar{C}_1\rangle$ /mol·dm^{-3}	$\langle\bar{C}_2\rangle$ /mol·dm^{-3}	$10^9(D_{11})_0$/m^2·s^{-1}	$10^9(D_{12})_0$/m^2·s^{-1}	$10^9(D_{21})_0$/m^2·s^{-1}	$10^9(D_{22})_0$/m^2·s^{-1}
			$\langle\bar{C}_T\rangle = 0.5$ mol·dm^{-3}			
1	0.49998	0	1.4885 ± 0.001	0.176 ± 0.015	0	0.906 ± 0.015
0.95	0.47493	0.02499	1.5151	0.1820	−0.0183	0.8878
0.90	0.45002	0.05000	1.5445	0.1970	−0.0384	0.8724
0.75	0.37499	0.12500	1.5894	0.1731	−0.0766	0.8499
0.50	0.25002	0.24998	1.6324	0.1443	−0.1238	0.8178
0.25	0.12499	0.37501_5	1.6629	0.0722	−0.1591	0.8069
0	0	0.50000	1.681 ± 0.002	0	−0.180 ± 0.006	0.8030 ± 0.001
0	0	0.50000	1.681 ± 0.002	0	−0.180 ± 0.006	0.8035 ± 0.001
			$\langle\bar{C}_T\rangle = 1.0$ mol·dm^{-3}			
1	1.00138	0	1.5118 ± 0.001	0.221 ± 0.015	0	0.858 ± 0.015
0.95	0.94960	0.04997	1.5152	0.2348	−0.0134	0.8315
0.90	0.90025_5	0.09999_5	1.5388	0.2540	−0.0319	0.8056
0.75	0.74990	0.24940	1.5599	0.2551	−0.0683	0.7545
0.50	0.49999	0.49996	1.5412	0.2036	−0.1005	0.7025
0.25	0.25000	0.74998	1.4801	0.1162	−0.1081	0.6779
0	0	0.99999	1.421 ± 0.027	0	−0.102 ± 0.021	0.6747 ± 0.001
0	0	1.00002	1.421 ± 0.027	0	−0.102 ± 0.021	0.6748 ± 0.001
			$\langle\bar{C}_T\rangle = 1.5$ mol·dm^{-3}			
1	1.50002	0	1.5448 ± 0.001	0.318 ± 0.015	0	0.808 ± 0.015
0.95	1.42493_5	0.07498	1.5485	0.3266	−0.0147	0.7780
0.90	1.34911	0.14990	1.5441	0.3330	−0.0258	0.7484
0.75	1.12447	0.37497	1.5317	0.3334	−0.0537	0.6835
0.50	0.74995	0.74996	1.4507	0.2790	−0.0688	0.6180
0.25	0.37505	1.12516	1.3062	0.1457	−0.0481	0.5994
0	0	1.50007	1.145 ± 0.02	0	−0.01 ± 0.02	0.6018 ± 0.001
0	0	1.50001	1.145 ± 0.02	0	−0.01 ± 0.02	0.6012 ± 0.001
			$\langle\bar{C}_T\rangle = 2.0$ mol·dm^{-3}			
1	1.99994	0	1.5884 ± 0.001	0.396	0	0.763 ± 0.015
0.95	1.89909	0.09994	1.5646	0.4235	-0.0089_5	0.7285
0.90	1.80007	0.19998	1.5563	0.4511	−0.0193	0.6937_5
			$\langle\bar{C}_T\rangle = 3.0$ mol·dm^{-3}			
1	3.00019	0	1.6682 ± 0.001	0.700	0	0.666 ± 0.015
0.95	2.84561	0.14976	1.6307	0.7023	−0.0033	0.6329
0.90	2.70025	0.30004	1.5968	0.7049	−0.0053	0.5996
			$\langle\bar{C}_T\rangle = 4.0$ mol·dm^{-3}			
1	4.00017_5	0	1.7457 ± 0.001	1.038	0	0.572 ± 0.015
0.95	3.78944_5	0.19943	1.6851_5	0.9898	0.0051	0.5491
0.90	3.60091_5	0.40010	1.6149	0.9422	0.0148	0.5264
			$\langle\bar{C}_T\rangle = 5.0$ mol·dm^{-3}			
1	4.99938	0	1.7912 ± 0.001	1.258	0	0.500 ± 0.015
0.95	4.72944	0.24890	1.7027	1.2183	0.0150	0.4804
0.90	4.50638	0.50070	1.6029_5	1.1798	0.0328	0.4603_5

[a] The values of $(D_{ij})_0$ of the mixtures. For the limiting case as $z_1 \rightarrow 1$, $(D_{11})_0 = D_0$ of NaCl(aq) at the same molar concentration, $(D_{21})_0 = 0$, $(D_{12})_0$ is an extrapolated value and $(D_{22})_0$ is an extrapolated value equal to the trace diffusion coefficient of SO_4^{2-} in NaCl(aq). Similarly, for the limiting case as $z_1 \rightarrow 0$, $(D_{22})_0 = D_0$ of Na_2SO_4(aq) at the same molar concentration, $(D_{12})_0 = 0$, $(D_{21})_0$ is an extrapolated value and $(D_{11})_0$ is an extrapolated value equal to the trace diffusion coefficient of the Cl^- ion in Na_2SO_4(aq).

to assess realistic uncertainties of the individual diffusion coefficients and therefore of the derived $(L_{ij})_0$ and $(L_{ij})_V$ values.

The experimental diffusion coefficients $(D_{ij})_V$ from these studies and their statistical standard errors[17−21] are summarized below in Table 1, as are the calculated $(D_{ij})_0$ in Table 2.

The μ_{ij} values are also needed for the calculation of $(L_{ij})_0$ and indirectly for $(L_{ij})_V$. They were obtained as follows.

Rard et al.[24] have represented the thermodynamic activities for the NaCl + Na_2SO_4 + H_2O system over the temperature range (278.15 to 318.15) K using an extended form of Pitzer's ion-interaction model.[25] This model includes the higher-order electrostatic term ${}^{E}\theta_{Cl,SO_4}(I)$ for unsymmetrical mixing of electrolytes, as described in Pitzer's Appendix B.[25] However, taking the concentration derivatives of the activity coefficient equations given in ref 24 will generate highly complicated expressions for μ_{ij}, in part because of the presence of this ${}^{E}\theta_{Cl,SO_4}(I)$ term.

On the other hand, Scatchard's neutral-electrolyte equation[26] is capable of representing thermodynamic activity data for ternary electrolyte mixtures very accurately, and general expressions for the four chemical-potential molality derivatives have been recently reported by Miller.[27] Thus, in this report we evaluate the neutral-electrolyte model parameters for the NaCl + Na_2SO_4 + H_2O system at 298.15 K. We then use the resulting chemical-potential molality derivatives calculated from this model (which are related to the corresponding activity coefficient molality derivatives), together with $\bar{V}_i$ to calculate μ_{ij}. These μ_{ij}, together with the experimental $(D_{ij})_V$ and derived $(D_{ij})_0$ values, allowed us to calculate the $(L_{ij})_V$ and $(L_{ij})_0$ values at all 23 compositions for which we previously reported diffusion coefficients and density data.[17−21] Uncertainties were assigned to the diffusion coefficients and activity coefficient derivatives. We then test the validity of the ORR at each composition using an expression[10,14] (eq 28 below), along with the experimental $(D_{ij})_V$, the activity coefficient derivatives, and their uncertainties, that yields a more direct test of the ORR[10] and minimizes the accumulation of errors from including unessential μ_{ij} terms that do not affect the test.

The goal of this analysis is to quantitatively test the ORR for ternary-solution diffusion using the extensive accurate diffusion coefficients and activity coefficient derivatives for the NaCl + Na_2SO_4 + H_2O system at 298.15 K for which realistic estimated uncertainties have been assigned. The calculations leave no doubt as to the validity of the ORR for this system over the investigated wide composition range.

Equations Used To Represent the Osmotic and Activity Coefficients of NaCl(aq), Na_2SO_4(aq) and Their Mixtures

Scatchard's neutral-electrolyte model[26] for a common-ion ternary mixture can be rewritten in the form

$$\begin{aligned}\phi^{S} &= \frac{\nu_1 m_1 \phi_1^{o}}{\sum_{i=1}^{2} \nu_i m_i} + \frac{\nu_2 m_2 \phi_2^{o}}{\sum_{i=1}^{2} \nu_i m_i} + \frac{I}{\sum_{i=1}^{2} \nu_i m_i}[y_1 y_2 (b_{01} I + b_{02} I^2 + b_{03} I^3) + y_1 y_2 (y_1 - y_2)(b_{12} I^2 + b_{13} I^3) + y_1 y_2 (y_1 - y_2)^2 b_{23} I^3] \\ &= h_1 \phi_1^{o} + h_2 \phi_2^{o} + \frac{I}{\sum_{i=1}^{2} \nu_i m_i}[y_1 y_2 (b_{01} I + b_{02} I^2 + b_{03} I^3) + y_1 y_2 (y_1 - y_2)(b_{12} I^2 + b_{13} I^3) + y_1 y_2 (y_1 - y_2)^2 b_{23} I^3] \quad (9)\end{aligned}$$

where ϕ_1^{o} and ϕ_2^{o} are the osmotic coefficients of the single-electrolyte solutions evaluated at the total stoichiometric ionic strength of the mixture; $\nu_1 m_1$ and $\nu_2 m_2$ are the ionic molalities ("osmolalities") of the two electrolytes assuming complete dissociation; I is the molality-based stoichiometric ionic strength of the mixture; y_1 and y_2 are the ionic strength fractions of the two electrolytes; and h_1 and h_2 are the ionic molality fractions ("osmolality fractions") of the electrolytes.

Although Scatchard[26] chose a particular extended Debye–Hückel equation to represent ϕ_i^{o}, there is nothing inherent in his approach that restricts it to his binary-solution equation. Pavićević et al.,[28] for example, represented their isopiestic results for mixtures with eq 9 while representing the binary solution ϕ_i^{o} contributions with the standard form of Pitzer's ion-interaction model,[25] and Miladinović et al.[29] used an extended form of this Pitzer model described by Archer[30] for ϕ_i^{o}. In these two studies,[28,29] the hybrid form of Scatchard's model using the ion-interaction binary-solution contributions gave a more accurate represention of the experimental osmotic coefficients than Pitzer's standard model for electrolyte mixtures. Consequently, we chose the hybrid model to represent the activity data for NaCl + Na_2SO_4 + H_2O.

Archer[30] and Rard et al.[24] used an extended form of Pitzer's ion-interaction model to represent the osmotic and activity coefficients of NaCl(aq) over a wide temperature range and of Na_2SO_4(aq) from T = (273.15 to 323.15) K, respectively. Their models represent these binary-solution thermodynamic properties very accurately and are accepted here. This extended ion-interaction equation for the osmotic coefficient of a solution of an electrolyte of arbitrary valence type can be written in the general form

$$\begin{aligned}\phi = 1 - |z_M z_X| A_\phi \left(\frac{I^{1/2}}{1 + bI^{1/2}}\right) + \left(\frac{2\nu_M \nu_X}{\nu}\right) m \{\beta_{M,X}^{(0)} + \beta_{M,X}^{(1)} \exp(-\alpha_{1,M,X} I^{1/2})\} + \left(\frac{4\nu_M^{\,2} \nu_X z_M}{\nu}\right) m^2 \{C_{M,X}^{(0)} + C_{M,X}^{(1)} \exp(-\omega_{1,M,X} I^{1/2})\} \quad (10)\end{aligned}$$

where A_ϕ is the Debye–Hückel limiting law slope for water; M denotes the cation and X the anion; z_M and z_X (with sign) are respectively the valences of the anion and cation; ν_M and ν_X are the stoichiometric ionization numbers of the anion and cation, respectively; $\nu = \nu_M + \nu_X$; b = 1.2 mol$^{-1/2}$·kg$^{1/2}$ is fixed for all aqueous electrolytes; and $\beta_{M,X}^{(i)}$ and $C_{M,X}^{(i)}$ are fitted empirical parameters that are determined using experimental data. The corresponding equation for the molality-based mean activity coefficient is

$$\begin{aligned}\ln \gamma_\pm = -|z_M z_X| A_\phi \left\{\left(\frac{I^{1/2}}{1 + bI^{1/2}}\right) + \left(\frac{2}{b}\right) \ln(1 + bI^{1/2})\right\} + \left(\frac{2\nu_M \nu_X}{\nu}\right) m \left[2\beta_{M,X}^{(0)} + \left(\frac{2\beta_{M,X}^{(1)}}{\alpha_{1,M,X}^{\,2} I}\right) \times \left\{1 - \left(1 + \alpha_{1,M,X} I^{1/2} - \frac{\alpha_{1,M,X}^{\,2} I}{2}\right) \exp(-\alpha_{1,M,X} I^{1/2})\right\}\right] + \left(\frac{2\nu_M^{\,2} \nu_X z_M}{\nu}\right) m^2 \left[3C_{M,X}^{(0)} + \left(\frac{4C_{M,X}^{(1)}}{\omega_{M,X}^{\,4} I^2}\right) \times \left\{6 - \left\{6 + 6\omega_{M,X} I^{1/2} + 3\omega_{M,X}^{\,2} I + \omega_{M,X}^{\,3} I^{3/2} - \left(\frac{\omega_{M,X}^{\,4} I^2}{2}\right)\right\} \exp(-\omega_{M,X} I^{1/2})\right\}\right] \quad (11)\end{aligned}$$

Table 3 lists the parameters of this model for NaCl(aq) and Na_2SO_4(aq) at 298.15 K. The parameters for Na_2SO_4(aq) were taken from the third column of Table 3 of Rard et al.[24] and those for NaCl(aq) were calculated from the equations and parameters reported by Archer.[30] The Debye–Hückel limiting law slope for water at T = 298.15 K and p = 0.1 MPa, A_ϕ = 0.391 475 mol$^{-1/2}$·kg$^{1/2}$, was calculated from the Archer and Wang evaluation.[31]

Rard et al.[24] based their temperature-dependent model for NaCl + Na_2SO_4 + H_2O on isopiestic data, Emfs from various types of cells, and enthalpies of mixing, whose data sources and assigned weights are summarized in their Table 2. However, the available isopiestic results were mainly restricted to 298.15 K; many of the Emf studies involved either sodium-ion-responsive glass electrodes or a so-called ion-selective electrode (none of which show a truly Nernstian response), and the enthalpies of mixing (although probably reliable) are mostly restricted to a few selected ionic strengths or equivalent molalities.

The most extensive isopiestic data for the NaCl + Na_2SO_4 + H_2O system were measured at 298.15 K, and this is the temperature at which we need to calculate values of μ_{ij}. We thus restricted the evaluation of the neutral-electrolyte model parameters to this temperature. There are four sets of isopiestic measurements at 298.15 K: 15 values from Wu et al.,[32] 4 from Robinson et al.,[33] 33 from Filippov and Cheremnykh,[34] and 119 values of Platford that are listed in Table 1 of Rard et al..[24] This last set is the most extensive and spans the full composition range from the dilute into the oversaturated (supersaturated) concentration region, I = (0.176 to 10.050) mol·kg^{-1}. The

Table 3. Parameters for the Extended Ion-Interaction (Pitzer) Models for Na_2SO_4(aq) and NaCl(aq) and the Debye−Hückel Limiting Law Slope, All at $T = 298.15$ K

	parameter value[a]	
parameter	Na_2SO_4(aq)	NaCl(aq)
$\beta^{(0)}_{M,X}$/mol^{-1}·kg	$9.1423 \cdot 10^{-3}$	0.080 634 21
$\beta^{(1)}_{M,X}$/mol^{-1}·kg	1.001 50	0.263 097 73
$C^{(0)}_{M,X}$/mol^{-2}·kg^2	$2.5960 \cdot 10^{-3}$	$2.6239 \cdot 10^{-4}$
$C^{(1)}_{M,X}$/mol^{-2}·kg^2	0.162 097	−0.010 051 73
$\alpha_{M,X}$/mol$^{-1/2}$·kg$^{1/2}$	2.0	2.0
$\omega_{M,X}$/mol$^{-1/2}$·kg$^{1/2}$	2.25	2.5
A_ϕ/mol$^{-1/2}$·kg$^{1/2}$	0.391 475	0.391 475
I_{max}/mol·kg^{-1}	11.44	6.15
$s(\phi)$	0.001 00	

[a] Parameters for Na_2SO_4(aq) were taken from Table 3 of Rard et al.,[24] and those for NaCl(aq) were calculated from the temperature and pressure coefficients reported by Archer.[30] The Debye−Hückel limiting law slope A_ϕ is from Archer and Wang.[31] I_{max} is the maximum ionic strength of the source data used for evaluation of the model parameters {the saturated solution for NaCl(aq) and oversaturated (supersaturated) solution for Na_2SO_4(aq)}.

analysis given by Rard et al.[24] indicates that the osmotic coefficients of Platford[24] and Robinson et al.[33] are completely consistent, whereas those of Filippov and Cheremnykh[34] are generally significantly lower and scattered, and those of Wu et al.[32] are systematically higher with the discrepancies becoming larger as the ionic strength fraction of Na_2SO_4 in the mixtures becomes larger. As noted by Rard et al., the binary-solution osmotic coefficients for Na_2SO_4(aq) from the study of Wu et al. are also systematically high, which implies that their[32] osmotic coefficients for the NaCl + Na_2SO_4 + H_2O mixtures are probably also systematically high and slightly skewed as a function of the NaCl solute fraction z_1.

On the basis of the considerations described in the preceding paragraph, evaluation of the b_{ij} mixing parameters of eq 9 was based on the two consistent sets of isopiestic data,[24,33] with equal weight given to each osmotic coefficient except for several points that were weighted zero by Rard et al.[24] Thus, 112 osmotic coefficients were used to evaluate the b_{ij} values. For these parameter evaluations, the quantity being minimized by least squares was $\Delta\phi = \phi(\text{expt}) - \phi^S$, where ϕ(expt) is an experimental osmotic coefficient and ϕ^S is an osmotic coefficient as given by Scatchard's neutral-electrolyte model, eq 9.

Table 4 gives the evaluated b_{ij} mixing parameters for 10 trial combinations of the b_{ij}, along with the ratio of the standard error of each coefficient divided by that coefficient's value (fractional errors) and the root-mean-square error for the fit RMSE(ϕ). As can be seen from Table 4 and from deviation plots (not shown in most cases), the one-parameter fit is not adequate and the two-parameter fits are fairly good but have small systematic deviations as a function of the ionic strength. Two of the three-parameter fits seem to be the best with essentially random deviations, and using four or more parameters gives no improvement in the RMSE(ϕ) value but merely results in larger standard coefficient errors. On the basis of RMSE(ϕ) and the standard coefficient errors, the two best (optimal) representations of the experimental osmotic coefficients are those involving two symmetrical mixing parameters and one asymmetrical one, $\{b_{01}, b_{02}, b_{13}\}$ and $\{b_{01}, b_{02}, b_{23}\}$, with $\{b_{01}, b_{02}, b_{23}\}$ having slightly better coefficient errors. The latter coefficient set is our recommended fit. Figure 1 is a deviation plot of ϕ(model) − ϕ(expt) against the ionic strength for the fit with the recommended $\{b_{01}, b_{02}, b_{23}\}$ parameter set.

We note that when eq 10 is used to represent ϕ_i^o of eq 9, replace m with I for NaCl(aq) and m with $I/3$ for Na_2SO_4(aq).

Calculation of the Chemical-Potential Derivatives μ_{ij} and μ^m_{ij} and the Concentration Derivatives $(\partial m_i/\partial C_j)_{p,T,C_{k(k\neq j)}}$

Equation 7 can be rewritten as

$$\mu_{ij} = \left(\frac{\partial G_i}{\partial C_j}\right)_{p,T} = \sum_{k=1}^{2} \left(\frac{\partial G_i}{\partial m_k}\right)_{p,T,C_{l(l\neq k)}} \left(\frac{\partial m_k}{\partial C_j}\right)_{p,T,C_{l(l\neq j)}} \quad (12)$$

We first consider the first partial differential on the right-hand side (RHS) of this equation and the relation between G_i and the molality and mean activity coefficient of solute component i when ideality is defined on the molality scale:

$$\mu^m_{ij} = \left(\frac{\partial G_i}{\partial m_j}\right)_{p,T} = \frac{\partial}{\partial m_j}\{G^o_{m,i} + RT \ln(\upsilon_{M_i}{}^{\upsilon_{M_i}} \upsilon_{X_i}{}^{\upsilon_{X_i}} m_i{}^{\upsilon_i} \gamma_{\pm,i}{}^{\upsilon_i})\}_{p,T} \quad (13)$$

where $R = 8.3145$ J·K^{-1}·mol^{-1} is the gas constant and T the absolute temperature. We now consider separately the two cases when $i \neq j$ and when $i = j$. For the first case,

$$\mu^m_{ij} = RT \frac{\partial}{\partial m_j}\{\ln(m_i{}^{\upsilon_i} \gamma_{\pm,i}{}^{\upsilon_i})\}_{p,T} = \upsilon_i RT \left\{\frac{\partial \ln \gamma_{\pm,i}}{\partial m_j}\right\}_{p,T}, \quad i \neq j \quad (14a)$$

and for the second case

$$\mu^m_{ii} = RT \frac{\partial}{\partial m_i}\{\ln(m_i{}^{\upsilon_i} \gamma_{\pm,i}{}^{\upsilon_i})\}_{p,T} = \upsilon_i RT \left(\frac{1}{m_i} + \left\{\frac{\partial \ln \gamma_{\pm,i}}{\partial m_i}\right\}_{p,T}\right) \quad (14b)$$

Miller[27] has recently reported explicit equations for $\{\partial \ln \gamma_{\pm,i}/\partial m_i\}_{p,T}$ and $\{\partial \ln \gamma_{\pm,i}/\partial m_j\}_{p,T}$ $(i \neq j)$ when Scatchard's neutral-electrolyte model, eq 9, is used to represent the osmotic and

Table 4. Mixing Parameter Values of Scatchard's Neutral-Electrolyte Equation for NaCl + Na_2SO_4 Aqueous Mixtures at $T = 298.15$ K, Using the Extended Ion-Interaction (Pitzer) Model Parameters for the Single Electrolytes Na_2SO_4(aq) and NaCl(aq) Reported in Table 3[a]

b_{01}/kg·mol^{-1}	b_{02}/kg^2·mol^{-2}	b_{03}/kg^3·mol^{-3}	b_{12}/kg^2·mol^{-2}	b_{13}/kg^3·mol^{-3}	b_{23}/kg^3·mol^{-3}	RMSE(ϕ)
−0.049 872 1 (0.0115)						0.002 95
−0.066 949 1 (0.0089)	0.003 055 1 (0.0329)					0.000 97
−0.058 607 7 (0.0084)		0.000 251 5 (0.0479)				0.001 33
−0.071 488 8 (0.0162)	0.004 879 6 (0.0861)	−0.000 162 9 (0.2246)				0.000 89
−0.068 940 6 (0.0097)	0.003 645 4 (0.0407)		0.000 585 5 (0.1988)			0.000 88
−0.069 849 1 (0.0103)	0.003 818 6 (0.0412)			0.000 085 4 (0.1706)		0.000 85
−0.069 153 5 (0.0092)	0.003 616 9 (0.0358)				−0.000 087 6 (0.1695)	0.000 85
−0.071 009 9 (0.0158)	0.004 534 8 (0.0923)	−0.000 093 9 (0.4410)	0.000 424 6 (0.3168)			0.000 86
−0.069 810 4 (0.0172)	0.003 799 3 (0.1331)	0.000 002 4 (24.90)		0.000 086 2 (0.2863)		0.000 85
−0.070 784 3 (0.0227)	0.004 690 4 (0.1934)	−0.000 138 7 (0.8711)	0.001 056 4 (0.6767)	−0.000 209 7 (0.8454)	−0.000 138 9 (0.5137)	0.000 84

[a] To the right of each parameter value, in parentheses, is given the ratio of the standard error of the b_{ij} coefficient divided by that coefficient (fractional error). RMSE(ϕ) is the root-mean-square error of the fit to the experimental osmotic coefficients.

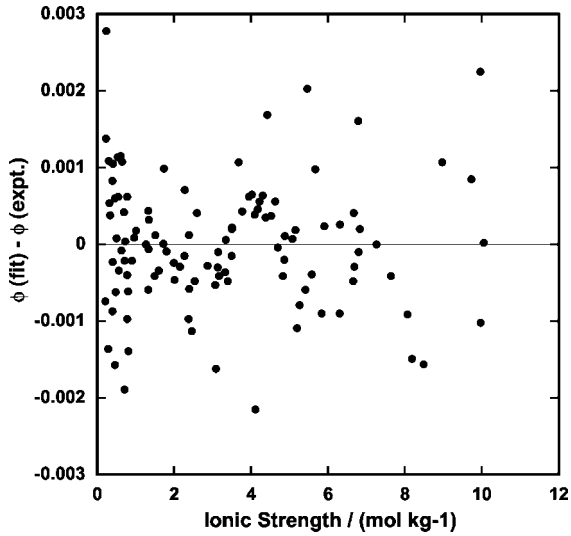

Figure 1. Deviations between the optimized Scatchard model values from eq 9 and the experimental osmotic coefficients, ϕ(fit) − ϕ(expt), as a function of the molality-based ionic strength I for the recommended $\{b_{01}, b_{02}, b_{23}\}$ parameter set of Table 4 and the binary-solution parameters of Table 3.

activity coefficients of ternary electrolyte solutions. This is the same model that we are using so we need not repeat those equations here. However, Miller's equations contain the derivative $\{\partial \ln \gamma^{o}_{\pm,i}/\partial I\}_{p,T}$, where $\gamma^{o}_{\pm,i}$ is the mean activity coefficient of electrolyte i in its *binary* solution at the total ionic strength I of the ternary mixture. This ionic strength derivative expression has not been reported previously for the extended ion-interaction (Pitzer) model used here, eq 11, and is therefore derived here.

Equation 11 as written is a function of both the stoichiometric ionic strength and the molality of electrolyte i, and it is more convenient to express it solely in terms of the ionic strength before taking the ionic strength derivative $\{\partial \ln \gamma^{o}_{\pm,i}/\partial I\}_{p,T}$. The molality and ionic strength of an electrolyte of arbitrary valence type are related by

$$m = \frac{2I}{v|z_M z_X|} \tag{15}$$

Inserting eq 15 into eq 11 yields

$$\ln \gamma^{o}_{\pm,i} = -|z_M z_X| A_\phi \left\{\left(\frac{I^{1/2}}{1+bI^{1/2}}\right) + \left(\frac{2}{b}\right)\ln(1+bI^{1/2})\right\} + \left(\frac{8v_M v_X}{v^2|z_M z_X|}\right)\left[\beta^{(0)}_{M,X} I + \left(\frac{\beta^{(1)}_{M,X}}{\alpha_{1,M,X}{}^2}\right)\left\{1-\left(1+\alpha_{1,M,X}I^{1/2} - \frac{\alpha_{1,M,X}{}^2 I}{2}\right)\exp(-\alpha_{1,M,X}I^{1/2})\right\}\right] + \left(\frac{8v_M{}^2 v_X}{v^3|z_M z_X{}^2|}\right)\left[3C^{(0)}_{M,X} I^2 + \left(\frac{4C^{(1)}_{M,X}}{\omega_{M,X}{}^4}\right)\times \left\{6 - \left\{6 + 6\omega_{M,X}I^{1/2} + 3\omega_{M,X}{}^2 I + \omega_{M,X}{}^3 I^{3/2} - \left(\frac{\omega_{M,X}{}^4 I^2}{2}\right)\right\}\times \exp(-\omega_{M,X}I^{1/2})\right\}\right] \tag{16}$$

The ionic strength derivative is then given by

$$\left\{\frac{\partial \ln \gamma^{o}_{\pm,i}}{\partial I}\right\}_{T,p} = -|z_M z_X| A_\phi \left\{\frac{1.5I^{1/2}+b}{(1+bI^{1/2})^2}\right\} + \left(\frac{8v_M v_X}{v^2|z_M z_X|}\right)\times \left\{\beta^{(0)}_{M,X} + \beta^{(1)}_{M,X}\left(1 - \frac{\alpha_{1,M,X}I^{1/2}}{4}\right)\exp(-\alpha_{1,M,X}I^{1/2})\right\} + \left(\frac{8v_M{}^2 v_X}{v^3|z_M z_X{}^2|}\right)\{6C^{(0)}_{M,X} I + C^{(1)}_{M,X}(6I - \omega_{M,X}I^{3/2})\exp(-\omega_{M,X}I^{1/2})\} \tag{17}$$

The remaining derivative on the RHS of eq 12 is the molality/molarity concentration derivative $(\partial m_i/\partial C_j)_{p,T,C_{k(k\neq j)}}$. Miller[10] gave equations for evaluating this derivative:

$$\left(\frac{\partial m_i}{\partial C_j}\right)_{p,T,C_{k(k\neq j)}} = \left(\frac{m_i}{C_j}\right)\left[\delta_{ij} + \frac{C_i \bar{V}_j}{C_0 \bar{V}_0}\right] = \left(\frac{1000}{C_0 M_0}\right)\left[\delta_{ij} + \frac{C_i \bar{V}_j}{C_0 \bar{V}_0}\right] = \left(\frac{1000}{C_0 M_0}\right) A^{0V}_{ij} \tag{18}$$

where $\bar{V}_j$ is the partial molar volume of solute j in the mixed electrolyte solution and $\bar{V}_0$ is the partial molar volume of the solvent (all in units of $cm^3 \cdot mol^{-1}$), $\delta_{ij} = 1$ if $i = j$ and $\delta_{ij} = 0$ if $i \neq j$ (δ_{ij} is the Kronecker δ), and A^{0V}_{ij} is defined by eq 18 and also in the Appendix.

Four experiments were performed at each overall composition in the diffusion studies for the NaCl + Na_2SO_4 + H_2O system,[17−21] each of which involved a pair of solutions, and thus eight density measurements were made. Also reported in these studies were the overall average molarities of both solute components for the four experiments, with the molalities corresponding to these average molarities and the partial molar volumes of the solutes and water at these overall average molarities. Therefore, all of the information needed to calculate the values of $(\partial m_i/\partial C_j)_{p,T,C_{k(k\neq j)}}$ are already available.

Table 5 reports the derived values of μ_{11}/RT, μ_{12}/RT, μ_{21}/RT, and μ_{22}/RT. They were evaluated by using the selected $\{b_{01}, b_{02}, b_{23}\}$ parameter set of Table 4 to calculate the values of $\mu^m_{ij} = (\partial G_i/\partial m_j)_{p,T}$ from eqs 14a and 14b, followed by the calculation of $(\partial m_i/\partial C_j)_{p,T,C_{k(k\neq j)}}$ by insertion of eq 18 into eq 12. The molality activity coefficient derivatives of eqs 14a and 14b are reported in Table 6. It should be noted that $\mu_{12} \neq \mu_{21}$ for the cross-term chemical-potential derivatives with respect to the *molarity* whereas for any thermodynamically consistent *molality*-based model for ternary electrolyte solutions,

$$\mu^m_{12} = \left(\frac{\partial G_1}{\partial m_2}\right)_{p,T} = \left(\frac{\partial G_2}{\partial m_1}\right)_{p,T} = \mu^m_{21} \tag{19}$$

Calculation of the $(D_{ij})_0$, $(L_{ij})_0$, μ_{ij}, μ^m_{ij}, and $(L_{ij})_V$ Values and of Tests of the ORR

The Appropriate Equations for Ternary Systems. The equations below[14] can be obtained most easily by matrix methods, as shown in the Appendix.

$(D_{ij})_0$ are obtained from $(D_{ij})_V$ from[14] (also see the Appendix)

$$(D_{ij})_0 = \sum_{k=1}^{2} \alpha_{ki}(D_{kj})_V = \sum_{k=1}^{2} A^{0V}_{ik}(D_{kj})_V \tag{20}$$

where

$$\alpha_{ij} = \delta_{ij} + \frac{C_j \bar{V}_i}{C_0 \bar{V}_0} = A_{ji}^{0V} \tag{21}$$

(See the Appendix for the meaning of $\tilde{A}_{ji}^{0V}$, which is the *transpose* of A_{ij}^{0V}.)

We also note that

$$\begin{aligned}\mu_{ij} &= \frac{1}{C_0 M_0}\sum_{k=1}^{2}\mu_{ik}^{m}\left(\delta_{kj} + \frac{C_k \bar{V}_j}{C_0 \bar{V}_0}\right)\\ &= \frac{1}{C_0 M_0}\sum_{k=1}^{2}\mu_{ik}^{m}\alpha_{jk}\\ &= \frac{1}{C_0 M_0}\sum_{k=1}^{2}\mu_{ik}^{m}A_{kj}^{0V}\end{aligned} \tag{22a}$$

where M_0 is the molar mass of the solvent (H_2O in our case) in units of kg·mol^{-1}. Explicit results for the cross derivatives are

$$\mu_{12} = \frac{1}{C_0 M_0}\left\{\mu_{11}^{m}\left(\frac{C_1 \bar{V}_2}{C_0 \bar{V}_0}\right) + \mu_{12}^{m}\left(1 + \frac{C_2 \bar{V}_2}{C_0 \bar{V}_0}\right)\right\} \tag{22b}$$

$$\mu_{21} = \frac{1}{C_0 M_0}\left\{\mu_{21}^{m}\left(1 + \frac{C_1 \bar{V}_1}{C_0 \bar{V}_0}\right) + \mu_{22}^{m}\left(\frac{C_2 \bar{V}_1}{C_0 \bar{V}_0}\right)\right\} \tag{22c}$$

Although the molality derivatives $\mu_{12}^{m} = \mu_{21}^{m}$ by eq 19, comparison of eq 22b with eq 22c shows that for the corresponding molarity derivatives $\mu_{12} \neq \mu_{21}$.

Expressions for $(L_{ij})_0$ can also be obtained by solution of the four expressions contained in eq 6 or by matrix inversion of eq 6. Either way, the results are[35]

$$(L_{11})_0 = 10^{-3}[(D_{11})_0 \mu_{22} - (D_{12})_0 \mu_{21}]/S \tag{23a}$$

$$(L_{12})_0 = 10^{-3}[(D_{12})_0 \mu_{11} - (D_{11})_0 \mu_{12}]/S \tag{23b}$$

$$(L_{21})_0 = 10^{-3}[(D_{21})_0 \mu_{22} - (D_{22})_0 \mu_{21}]/S \tag{23c}$$

$$(L_{22})_0 = 10^{-3}[(D_{22})_0 \mu_{11} - (D_{21})_0 \mu_{12}]/S \tag{23d}$$

where

$$S = \mu_{11}\mu_{22} - \mu_{12}\mu_{21} \tag{24}$$

The factor 10^{-3} appears in these equations because of SI units of m^2·s^{-1} for $(D_{ij})_0$ and mol·dm^{-3} for molar concentrations.

Similarly, expressions for $(L_{ij})_V$ are obtained by solving the four expressions contained in the volume-fixed analogue of eq 6 (see the Appendix). The results are[10,14]

$$(L_{11})_V = [(D_{11})_V a_{22} - (D_{12})_V a_{12}]/A \tag{25a}$$

$$(L_{12})_V = [(D_{12})_V a_{11} - (D_{11})_V a_{21}]/A \tag{25b}$$

$$(L_{21})_V = [(D_{21})_V a_{22} - (D_{22})_V a_{12}]/A \tag{25c}$$

$$(L_{22})_V = [(D_{22})_V a_{11} - (D_{21})_V a_{21}]/A \tag{25d}$$

where

$$a_{ij} = \sum\nolimits_{k=1}^{2}\alpha_{jk}\mu_{ki} \tag{26}$$

and

$$A = a_{11}a_{22} - a_{12}a_{21} \tag{27}$$

The $(D_{ij})_V$, $(D_{ij})_0$, μ_{ij}, $\{\partial \ln \gamma_{\pm,i}/\partial m_j\}_{p,T}$, $(L_{ij})_V$, and $(L_{ij})_0$ values respectively are contained in Tables 1, 2, and 5 to 8.

Table 5. Values of μ_{11}/RT, μ_{12}/RT, μ_{21}/RT, and μ_{22}/RT at $T = 298.15$ K at Each of the Mean Concentrations Used in the Diffusion Studies,[17−21] Calculated by Using the Selected $\{b_{01}, b_{02}, b_{23}\}$ Parameter Set of Table 4 and the Binary-Solution Parameters of Table 3[a]

z_1	$\langle\bar{C}_1\rangle$ /mol·dm^{-3}	$\langle\bar{C}_2\rangle$ /mol·dm^{-3}	(μ_{11}/RT)/dm^3·mol^{-1}	(μ_{12}/RT)/dm^3·mol^{-1}	(μ_{21}/RT)/dm^3·mol^{-1}	(μ_{22}/RT)/dm^3·mol^{-1}
			$\langle\bar{C}_T\rangle = 0.5$ mol·dm^{-3}			
0.95	0.47493	0.02499	3.80934	2.44097	2.44702	42.61239
0.90	0.45002	0.05000	3.87346	2.37606	2.38001	22.58730
0.75	0.37499	0.12500	4.17786	2.18170	2.18472	10.45933
0.50	0.25002	0.24998	5.32675	1.90553	1.90482	6.17388
0.25	0.12499	0.37501_5	9.19093	1.68573	1.68571	4.56691
			$\langle\bar{C}_T\rangle = 1.0$ mol·dm^{-3}			
0.95	0.94960	0.04997	2.02792	1.23170	1.22706_5	20.93400
0.90	0.90025_5	0.09999_5	2.06340	1.20661	1.20375	10.93678
0.75	0.74990	0.24940	2.22611	1.13741_5	1.13178_5	4.94385
0.50	0.49999	0.49996	2.81439	1.03247	1.02369	2.86029
0.25	0.25000	0.74998	4.75789	0.95309	0.93957	2.11226
			$\langle\bar{C}_T\rangle = 1.5$ mol·dm^{-3}			
0.95	1.42493_5	0.07498	1.45466	0.88163	0.87290_5	13.83882_5
0.90	1.34911	0.14990	1.48217	0.87404	0.86431	7.19708
0.75	1.12447	0.37497	1.59774	0.84599	0.83303	3.22139
0.50	0.74995	0.74996	2.00106	0.80271	0.78402	1.87872
0.25	0.37505	1.12516	3.30692	0.76988	0.74592	1.40945
			$\langle\bar{C}_T\rangle = 2.0$ mol·dm^{-3}			
0.95	1.89909	0.09994	1.18112	0.73884	0.72478	10.37087
0.90	1.80007	0.19998	1.20317	0.73910_5	0.72318	5.39176
			$\langle\bar{C}_T\rangle = 3.0$ mol·dm^{-3}			
0.95	2.84561	0.14976	0.92912	0.64890	0.62348	7.02213
0.90	2.70025	0.30004	0.94702	0.65832	0.63081_5	3.70346
			$\langle\bar{C}_T\rangle = 4.0$ mol·dm^{-3}			
0.95	3.78944_5	0.19943	0.82372	0.65153_5	0.61600	5.45450
0.90	3.60091_5	0.40010	0.84063	0.66991	0.63075	2.96678
			$\langle\bar{C}_T\rangle = 5.0$ mol·dm^{-3}			
0.95	4.72944	0.24890	0.77712_5	0.69453	0.64663	4.60689
0.90	4.50638	0.50070	0.79544	0.72103_5	0.67090	2.61550

[a] The values of μ_{ij}/RT are given to the number of figures used for the calculation of $(L_{ij})_0$ and $(L_{ij})_V$. Although these values are reported to several more figures than justified by their absolute accuracy, we retained extra figures in the calculations to avoid round-off errors because various combinations of μ_{ij} are involved in the calculations, e.g., $(\mu_{11}\mu_{22} - \mu_{12}\mu_{21})$.

The $(L_{ij})_V$ values of Table 7 are those based on the volume-fixed driving force defined to be consistent with the invariance of entropy production.[4,10,14]

The ORR can be tested directly by comparing L_{12} and L_{21} on either reference frame calculated from the appropriate equations given above, using the D_{ij}, $\bar{V}_i$, and μ_{ij} values. However, the L_{ij} expressions in terms of D_{ij} and μ_{ij} have many extraneous terms including the determinants from matrix inversions, as can be inferred from eq 6. These extraneous terms contribute to the estimated error from the propagation-of-errors equations, yet they are unessential in comparing L_{12} with L_{21}.

An alternative test of the ORR can eliminate or simplify some of these terms by various transformations that give necessary and sufficient conditions for the ORR. The simpler test equation[10,14] is advantageous because it cancels out just those terms on both sides of that equation that would otherwise make irrelevant contributions to the estimated error.

It is also desirable to use the volume-fixed $(D_{ij})_V$ directly for this test because they are the experimental quantities, whereas the solvent-fixed $(D_{ij})_0$ require additional $\bar{V}_i$ terms along with their own (small) experimental errors.

Thus, the simpler ORR test equation for a ternary system is[10,14]

$$a_{11}(D_{12})_V + a_{12}(D_{22})_V = a_{21}(D_{11})_V + a_{22}(D_{21})_V \quad (28)$$

This test condition is derived by equating eq 25b to eq 25c and requires that the denominator of these equations be nonzero, i.e., $A \neq 0$.

The RHS, left-hand side (LHS), RHS − LHS, and its uncertainty of this test equation are given in Table 9.

Estimates of the Errors in Experimental Quantities

To estimate the fractional uncertainties in the activity coefficient derivatives for the selected best fit with $\{b_{01}, b_{02}, b_{23}\}$, the $(\partial \ln \gamma_{\pm,i}/\partial m_j)_{p,T} = (1/\gamma_{\pm,i})(\partial \gamma_{\pm,i}/\partial m_j)_{p,T}$ values were also calculated for two other sets of parameters from Table 4 for fits with low and comparable RMSE(ϕ): $\{b_{01}, b_{02}, b_{13}\}$ and $\{b_{01}, b_{02}, b_{03}, b_{12}, b_{13}, b_{23}\}$. The maximum differences among these three sets of calculated $(\partial \ln \gamma_{\pm,i}/\partial m_j)_{p,T}$ values at each composition, $\Delta(\partial \ln \gamma_{\pm,i}/\partial m_j)_{p,T}$, are reported in Table 6.

Inspection of the $\Delta(\partial \ln \gamma_{\pm,i}/\partial m_j)_{p,T}$ in Table 6 shows some obvious trends. (i) Values of all three of the $\Delta(\partial \ln \gamma_{\pm,i}/\partial m_j)_{p,T}$ for a fixed z_1 solute ratio continually increase with increasing total concentration $\langle \bar{C}_T \rangle$. (ii) At any fixed value of $\langle \bar{C}_T \rangle$, the values of $\Delta(\partial \ln \gamma_{\pm,1}/\partial m_1)_{p,T}$ are smaller as $z_1 \rightarrow 1$ and larger as $z_1 \rightarrow 0$. Thus, the NaCl derivative is more accurate as the NaCl(aq) binary composition is approached and least accurate

Table 6. Values of $(\partial \ln \gamma_{\pm,i}/\partial m_j)_{p,T}$ at $T = 298.15$ K at Each of the Mean Concentrations and the Corresponding Molalities Used in the Diffusion Studies,[17−21] Calculated by Using the Selected $\{b_{01}, b_{02}, b_{23}\}$ Parameter Set of Table 4 and the Binary-Solution Parameters of Table 3, and Maximum Differences among Values from Three Mixing Parameter Sets[a]

z_1	$\langle \bar{C}_1 \rangle$ / mol·dm^{-3}	$\langle \bar{C}_2 \rangle$ / mol·dm^{-3}	$(\partial \ln \gamma_{\pm,1}/\partial m_1)_{p,T}$ / kg·mol^{-1}	$v_1(\partial \ln \gamma_{\pm,1}/\partial m_2)_{p,T}$ / kg·mol^{-1}	$(\partial \ln \gamma_{\pm,2}/\partial m_2)_{p,T}$ / kg·mol^{-1}	$m_1(\bar{C}_1,\bar{C}_2)$ and $m_2(\bar{C}_1,\bar{C}_2)$ / mol·kg^{-1}
			$\langle \bar{C}_T \rangle = 0.5$ mol·dm^{-3}			
0.95	0.47493	0.02499	−0.11678 (0.00006)	−1.38813 (0.00212)	−1.66658 0.00026)	0.480654 0.025296
0.90	0.45002	0.05000	−0.09977 (0.00014)	−1.28227 (0.00227)	−1.55758 (0.00025)	0.455455 0.050605
0.75	0.37499	0.12500	−0.06138 (0.00033)	−1.04351 (0.00271)	−1.31214 (0.00019)	0.379555 0.126524
0.50	0.25002	0.24998	−0.02081 (0.00070)	−0.79215 (0.00341)	−1.05543 (0.00014)	0.253120 0.253075
0.25	0.12499	0.37501_5	0.00546 (0.00108)	−0.63116 (0.00407)	−0.89310 (0.00007)	0.126579 0.379785
			$\langle \bar{C}_T \rangle = 1.0$ mol·dm^{-3}			
0.95	0.94960	0.04997	−0.00824 (0.00010)	−0.70622 (0.00123)	−0.95979 (0.00052)	0.970554 0.051071
0.90	0.90025_5	0.09999_5	0.00197 (0.00021)	−0.64340 (0.00123)	−0.89690 (0.00047)	0.920260 0.102217
0.75	0.74990	0.24940	0.02536 (0.00055)	−0.50097 (0.00138)	−0.75622 (0.00037)	0.767013 0.255091
0.50	0.49999	0.49996	0.05187 (0.00119)	−0.34325 (0.00227)	−0.60467 (0.00023)	0.512051 0.512020
0.25	0.25000	0.74998	0.07026 (0.00191)	−0.23766 (0.00331)	−0.50649 (0.00014)	0.256408 0.769204
			$\langle \bar{C}_T \rangle = 1.5$ mol·dm^{-3}			
0.95	1.42493_5	0.07498	0.03584 (0.00010)	−0.42975 (0.00199)	-0.67698_5 (0.00078)	1.471642 0.077436
0.90	1.34911	0.14990	0.04370 (0.00022)	−0.38247 (0.00180)	−0.63206 (0.00070)	1.393896 0.154878
0.75	1.12447	0.37497	0.06259 (0.00062)	−0.27065 (0.00115)	-0.52814_5 (0.00050)	1.163458 0.387972
0.50	0.74995	0.74996	0.08476 (0.00145)	−0.14440 (0.00148)	−0.41539 (0.00029)	0.778110 0.778118
0.25	0.37505	1.12516	0.10096 (0.00260)	−0.05742 (0.00263)	−0.34042 (0.00020)	0.390373 1.171128
			$\langle \bar{C}_T \rangle = 2.0$ mol·dm^{-3}			
0.95	1.89909	0.09994	0.06179 (0.00013)	−0.26738 (0.00266)	−0.51349 (0.00103)	1.982979 0.104356
0.90	1.80007	0.19998	0.06866 (0.00025)	−0.22672 (0.00212)	−0.47715 (0.00100)	1.881053 0.208973
			$\langle \bar{C}_T \rangle = 3.0$ mol·dm^{-3}			
0.95	2.84561	0.14976	0.09306 (0.00037)	−0.07028 (0.00370)	−0.31746 (0.00291)	3.041664 0.160075
0.90	2.70025	0.30004	0.09892 (0.00066)	−0.03584 (0.00251)	−0.29081 (0.00244)	2.891262 0.321261
			$\langle \bar{C}_T \rangle = 4.0$ mol·dm^{-3}			
0.95	3.78944_5	0.19943	0.11222 (0.00092)	0.05427 (0.00863)	−0.19324 (0.00550)	4.153577 0.218593
0.90	3.60091_5	0.40010	0.11762 (0.00172)	0.08681 (0.00735)	−0.17203 (0.00466)	3.959282 0.439914
			$\langle \bar{C}_T \rangle = 5.0$ mol·dm^{-3}			
0.95	4.72944	0.24890	0.12566 (0.00176)	0.14576 (0.02101)	−0.09993 (0.00911)	5.324414 0.280213
0.90	4.50638	0.50070	0.13090 (0.00332)	0.17907 (0.01862)	−0.08204 (0.00780)	5.098715 0.566518

[a] The values of $(\partial \ln \gamma_{\pm,i}/\partial m_j)_{p,T}$ are given to the number of figures used for the calculation of $(L_{ij})_0$ and $(L_{ij})_V$. Although these values are reported to several more figures than justified by their absolute accuracy, we retained extra figures in the calculations to avoid round-off errors. There are three tabulated derivatives given for each composition. Only the one cross derivative v_1 $(\partial \ln \gamma_{\pm,1}/\partial m_2)_{p,T}$ is necessary because of the equality v_1 $(\partial \ln \gamma_{\pm,1}/\partial m_2)_{p,T} = v_2$ $(\partial \ln \gamma_{\pm,2}/\partial m_1)_{p,T}$, which comes from $\mu^m_{12} = \mu^m_{21}$. The uncertainties, $\Delta(\partial \ln \gamma_{\pm,i}/\partial m_j)_{p,T}$, given in parentheses to the right of the corresponding $(\partial \ln \gamma_{\pm,i}/\partial m_j)_{p,T}$ from the selected $\{b_{01}, b_{02}, b_{23}\}$ parameter set, are the maximum differences among the values calculated for three sets of parameters from Table 4 with low and comparable RMSE(ϕ): $\{b_{01}, b_{02}, b_{23}\}$, $\{b_{01}, b_{02}, b_{13}\}$, and $\{b_{01}, b_{02}, b_{03}, b_{12}, b_{13}, b_{23}\}$.

Table 7. Values of the Volume-Fixed Onsager Diffusion Coefficients $(L_{ij})_V$ at $T = 298.15$ K at Each of the Mean Concentrations Used in the Diffusion Studies[a]

composition[b]	$10^{12}RT(L_{11})_V$ / mol·m^{-1}·s^{-1}	$10^{12}RT(L_{12})_V$ / mol·m^{-1}·s^{-1}	$10^{12}RT(L_{21})_V$ / mol·m^{-1}·s^{-1}	$10^{12}RT(L_{22})_V$ / mol·m^{-1}·s^{-1}
		$\langle\bar{C}_T\rangle = 0.5$ mol·dm^{-3}		
1	0.403	−0.019	−0.019	0.022
2	0.414	−0.036	−0.036	0.042
3	0.412	−0.072	−0.069	0.095
4	0.333	−0.082	−0.081	0.156
5	0.190	−0.056	−0.055	0.194
		$\langle\bar{C}_T\rangle = 1.0$ mol·dm^{-3}		
6	0.741	−0.035	−0.033	0.042
7	0.757	−0.065	−0.064	0.080
8	0.745	−0.129	−0.127	0.180
9	0.592	−0.152	−0.151	0.293
10	0.327	−0.099	−0.100	0.351
		$\langle\bar{C}_T\rangle = 1.5$ mol·dm^{-3}		
11	1.032	−0.048	−0.048	0.059
12	1.038	−0.091	−0.089	0.114
13	1.009	−0.182	−0.178	0.254
14	0.783	−0.209	−0.211	0.401
15	0.420	−0.139	−0.137	0.466
		$\langle\bar{C}_T\rangle = 2.0$ mol·dm^{-3}		
16	1.258	−0.060	−0.057	0.074
17	1.263	−0.111	−0.110	0.142
		$\langle\bar{C}_T\rangle = 3.0$ mol·dm^{-3}		
18	1.592	−0.076	−0.078	0.096
19	1.583	−0.143	−0.147	0.183
		$\langle\bar{C}_T\rangle = 4.0$ mol·dm^{-3}		
20	1.766	−0.086	−0.092	0.109
21	1.736	−0.171	−0.170	0.206
		$\langle\bar{C}_T\rangle = 5.0$ mol·dm^{-3}		
22	1.804	−0.099	−0.101	0.115
23	1.740	−0.179	−0.183	0.210

[a] $R = 8.3145$ J·K^{-1}·mol^{-1} and $T = 298.15$ K. These $(L_{ij})_V$ values are those calculated using the driving force defined to be consistent with the invariance of entropy production.[4,10] [b] The numbers in this column denote the compositions as defined in Table 1.

Table 8. Values of the Solvent-Fixed Onsager Diffusion Coefficients $(L_{ij})_0$ at $T = 298.15$ K at Each of the Mean Concentrations Used in the Diffusion Studies[a]

composition[b]	$10^{12}RT(L_{11})_0$ / mol·m^{-1}·s^{-1}	$10^{12}RT(L_{12})_0$ / mol·m^{-1}·s^{-1}	$10^{12}RT(L_{21})_0$ / mol·m^{-1}·s^{-1}	$10^{12}RT(L_{22})_0$ / mol·m^{-1}·s^{-1}
		$\langle\bar{C}_T\rangle = 0.5$ mol·dm^{-3}		
1	0.410	−0.019	−0.019	0.022
2	0.421	−0.036	−0.036	0.042
3	0.417	−0.070	−0.068	0.095
4	0.335	−0.080	−0.079	0.157
5	0.191	−0.055	−0.053	0.196
		$\langle\bar{C}_T\rangle = 1.0$ mol·dm^{-3}		
6	0.768	−0.034	−0.032	0.042
7	0.783	−0.063	−0.062	0.081
8	0.764	−0.124	−0.123	0.181
9	0.601	−0.146	−0.144	0.298
10	0.330	−0.094	−0.095	0.364
		$\langle\bar{C}_T\rangle = 1.5$ mol·dm^{-3}		
11	1.092	−0.046	−0.046	0.059
12	1.092	−0.086	−0.084	0.114
13	1.048	−0.172	−0.167	0.256
14	0.801	−0.194	−0.196	0.413
15	0.424	−0.128	−0.126	0.494
		$\langle\bar{C}_T\rangle = 2.0$ mol·dm^{-3}		
16	1.359	−0.056	−0.053	0.074
17	1.355	−0.102	−0.102	0.143
		$\langle\bar{C}_T\rangle = 3.0$ mol·dm^{-3}		
18	1.800	−0.066	−0.068	0.096
19	1.769	−0.124	−0.129	0.185
		$\langle\bar{C}_T\rangle = 4.0$ mol·dm^{-3}		
20	2.097	−0.069	−0.076	0.110
21	2.026	−0.140	−0.139	0.209
		$\langle\bar{C}_T\rangle = 5.0$ mol·dm^{-3}		
22	2.254	−0.075	−0.077	0.116
23	2.130	−0.136	−0.140	0.215

[a] $R = 8.3145$ J·K^{-1}·mol^{-1} and $T = 298.15$ K. [b] The numbers in this column denote the compositions as defined in Table 1.

as its trace composition is approached, which is an expected result. Correspondingly, at any fixed value of $\langle\bar{C}_T\rangle$, the values of $\Delta(\partial \ln \gamma_{\pm,2}/\partial m_2)_{p,T}$ are smaller as $z_1 \rightarrow 0$ and larger as $z_1 \rightarrow 1$. Thus, the Na_2SO_4 derivative is more accurate as the Na_2SO_4(aq) binary composition is approached and least accurate as its trace composition is approached. (iii) The uncertainty of the cross-derivative $\Delta(\partial \ln \gamma_{\pm,1}/\partial m_2)_{p,T}$ increases as $z_1 \rightarrow 0$ at $\langle\bar{C}_T\rangle = 0.5$ mol·dm^{-3}, is initially constant and then increases as $z_1 \rightarrow 0$ at $\langle\bar{C}_T\rangle = 1.0$ mol·dm^{-3}, but goes through a minimum at $\langle\bar{C}_T\rangle = 1.5$ mol·dm^{-3} with increasing values as $z_1 \rightarrow 0$ and $z_1 \rightarrow 1$.

The corresponding fractional uncertainties are not an ideal way of describing these differences because both $(\partial \ln \gamma_{\pm,1}/\partial m_1)_{p,T}$ and $(\partial \ln \gamma_{\pm,1}/\partial m_2)_{p,T}$ change sign (and thus must be zero at some mixture compositions), but the absolute values of their errors are used in this paragraph because it is a convenient way of assigning uncertainties needed for the $(L_{ij})_0$ and $(L_{ij})_V$ calculations. The values of the fractional uncertainties $F_{ij} = \{\Delta(\partial \ln \gamma_{\pm,i}/\partial m_j)_{p,T}/(\partial \ln \gamma_{\pm,i}/\partial m_j)_{p,T}\}$ are nearly always ≤ 0.03 when $\langle\bar{C}_T\rangle \leq 3.0$ mol·dm^{-3}, with the individual F_{ij} values usually being well below 0.02. However, $F_{11} \approx 0.20$ at $\langle\bar{C}_T\rangle = 0.5$ mol·dm^{-3} when $z_1 = 0.25$ and $F_{11} \approx 0.11$ at $\langle\bar{C}_T\rangle = 1.0$ mol·dm^{-3} when $z_1 = 0.90$, although the actual errors are very small in both cases because the values of $(\partial \ln \gamma_{\pm,1}/\partial m_1)_{p,T}$ are near zero. In addition, at $\langle\bar{C}_T\rangle = (4.0$ and $5.0)$ mol·dm^{-3} the values of F_{ij} may exceed 0.10 at some compositions and F_{12} at $\langle\bar{C}_T\rangle = 3.0$ mol·dm^{-3} reaches 0.07 mol·dm^{-3} when $z_1 = 0.90$.

We note that the ϕ_1^o and ϕ_2^o equations[24,30] used for the binary-solution contributions to eq 9 are the same for all of the derivative calculations and thus do not contribute to the observed variations from using different mixing parameter combinations. However, the errors in the derivatives of those binary-solution models do contribute to the overall errors in $(\partial \ln \gamma_{\pm,i}/\partial m_j)_{p,T}$. We have not estimated any errors of the binary-solution derivatives, although the uncertainties in the NaCl(aq) model may contribute somewhat at the highest concentrations that are near its fitting (solubility) limit. Because the ϕ_1^o equation[30] used here for NaCl(aq) was also used as the reference standard for the NaCl + Na_2SO_4 + H_2O mixtures[24] and was the standard for much of the Na_2SO_4(aq) isopiestic data, the binary- and ternary-solution osmotic and activity coefficient equations used in our $(\partial \ln \gamma_{\pm,i}/\partial m_j)_{p,T}$ calculations should be highly consistent internally.

The larger uncertainties of the $(\partial \ln \gamma_{\pm,i}/\partial m_j)_{p,T}$ values when $\langle\bar{C}_T\rangle = (4.0$ and $5.0)$ mol·dm^{-3} are not surprising because the isopiestic data used for evaluation[24] of the b_{ij} parameters of Table 4 extend only to the total molalities of $m_T \approx 3.8$ mol·kg^{-1}, with only a few points above $m_T \approx 3.6$ mol·kg^{-1}. However, the ionic strengths of the more concentrated isopiestic solutions do extend above those of the diffusion experiments (which are restricted to the NaCl-rich region with $z_1 = 0.90$ and 0.95) and provide some constraint on eq 9 at high concentrations, as do the binary-solution contributions that are valid to higher ionic strengths than the diffusion compositions.

After considering the issues described in the above discussion, we conservatively assign 0.05 uncertainties to the calculated F_{ij} when $\langle\bar{C}_T\rangle \leq 3.0$ mol·dm^{-3}, except for F_{12} at $\langle\bar{C}_T\rangle = 3.0$ mol·dm^{-3}, where the uncertainties may reach 0.10, and for F_{11}, where the uncertainty is ≈ 0.20 at $\langle\bar{C}_T\rangle = 0.5$ mol·dm^{-3} when

Table 9. Tests of the ORR at $T = 298.15$ K Using Equation 28[a]

composition[b]	10^{12}LHS/m^5·mol^{-1}·s^{-1}	10^{12}RHS/m^5·mol^{-1}·s^{-1}	10^{12}(LHS − RHS)/m^5·mol^{-1}·s^{-1}	10^{12}(uncertainty)/m^5·mol^{-1}·s^{-1}
		$\langle\bar{C}_T\rangle = 0.5$ mol·dm^{-3}		
1	2.865_7	2.918_6	−0.053	±0.220
2	2.839_3	2.803_1	+0.036	±0.125
3	2.580_1	2.666_6	−0.087	±0.161
4	2.326_6	2.346_2	−0.020	±0.220
5	2.023_9	2.076_7	−0.053	±0.321
		$\langle\bar{C}_T\rangle = 1.0$ mol·dm^{-3}		
6	1.496_4	1.587_1	−0.091	±0.110
7	1.493_9	1.508_0	−0.014	±0.059
8	1.421_8	1.436_7	−0.015	±0.073
9	1.292_3	1.303_7	−0.011	±0.033
10	1.189_6	1.182_2	+0.007	±0.039
		$\langle\bar{C}_T\rangle = 1.5$ mol·dm^{-3}		
11	1.154_1	1.162_5	−0.008	±0.072
12	1.140_4	1.163_9	−0.023	±0.036
13	1.102_1	1.122_7	−0.021	±0.028
14	1.042_9	1.035_2	+0.008	±0.021
15	0.929_0	0.937_9	−0.009	±0.017
		$\langle\bar{C}_T\rangle = 2.0$ mol·dm^{-3}		
16	1.028_3	1.063_5	−0.035	±0.053
17	1.044_5	1.046_0	−0.002	±0.025
		$\langle\bar{C}_T\rangle = 3.0$ mol·dm^{-3}		
18	1.047_0	1.035_2	+0.012	±0.020
19	1.045_8	1.031_6	+0.014	±0.012
		$\langle\bar{C}_T\rangle = 4.0$ mol·dm^{-3}		
20	1.153_6	1.126_2	+0.027	±0.031
21	1.124_0	1.125_8	−0.002	±0.032
		$\langle\bar{C}_T\rangle = 5.0$ mol·dm^{-3}		
22	1.257_4	1.251_7	+0.006	±0.049
23	1.247_4	1.241_3	+0.006	±0.052

[a] $R = 8.3145$ J·K^{-1}·mol^{-1} and $T = 298.15$ K. These reported quantities from eq 28 are LHS = $\{a_{11}(D_{12})_V + a_{12}(D_{22})_V\}/RT$ and RHS = $\{a_{21}(D_{11})_V + a_{22}(D_{21})_V\}/RT$. If the ORR for isothermal diffusion in a ternary system is obeyed, then LHS and RHS are equal within the uncertainties of determination of these quantities. [b] The numbers in this column denote the compositions as defined in Table 1.

$z_1 = 0.25$ and is ≈0.11 at $\langle\bar{C}_T\rangle = 1.0$ mol·dm^{-3} when $z_1 = 0.90$. Also, 0.10 uncertainties are assumed for F_{ij} at $\langle\bar{C}_T\rangle =$ (4.0 and 5.0) mol·dm^{-3}.

For the errors in the experimental-based $(D_{ij})_V$, we first examined plots of these values as a function of z_1 at constant $\langle\bar{C}_T\rangle = (0.5, 1.0, \text{and } 1.5)$ mol·dm^{-3}; at higher concentrations, such plots are less informative because the diffusion data are limited to a narrow range of z_1. These plots, given in Figures 1 and 2 of ref 19, are generally smooth, but the value of $(D_{12})_V$ at $\langle\bar{C}_T\rangle = 0.5$ mol·dm^{-3} and $z_1 = 0.75$ seems low by $0.03 \cdot 10^{-9}$ m^2·s^{-1}, and we thus assigned it this uncertainty. Plots of $(D_{21})_V$ and $(D_{11})_V$ as a function of $\langle\bar{C}_T\rangle$ showed no significant scatter at $z_1 = 0.90$ but were significantly scattered at $z_1 = 0.95$. These plots (not shown) indicate that, at $z_1 = 0.95$, $(D_{21})_V$ is uncertain by ± $0.004 \cdot 10^{-9}$ m^2·s^{-1} from $\langle\bar{C}_T\rangle = (0.5 \text{ to } 2.0)$ mol·dm^{-3} and by about ± $0.002 \cdot 10^{-9}$ m^2·s^{-1} at higher concentrations. The corresponding $(D_{11})_V$ plot at $z_1 = 0.95$ indicated a scatter of about ± $0.006 \cdot 10^{-9}$ m^2·s^{-1}. The coefficients $(D_{12})_V$ and $(D_{22})_V$ at constant z_1 show too much variation with the concentration to show scatter of this size. However, by a comparison of the statistical uncertainties in $(D_{ij})_V$ and the results from subset analysis,[17−21] we estimate that $\delta(D_{12})_V \approx 4\delta(D_{21})_V$ and $\delta(D_{22})_V \approx (1/2)\delta(D_{11})_V$. These uncertainty estimates were accepted. At all of the other compositions, we accepted the earlier "rule-of-thumb" that uncertainties in diffusion coefficients are roughly 4 times the statistical errors calculated by the propagation-of-errors method.[11,36]

Variation of the Diffusion Onsager Coefficients with the Solute Concentration and Equivalent Fraction

As seen from the information listed in Tables 7 and 8, the values of $(L_{11})_R$ and $(L_{22})_R$ in both reference frames are all positive, whereas the cross-terms $(L_{12})_R$ and $(L_{21})_R$ are all negative. As expected, the values of $(L_{11})_V$, $(L_{22})_V$, $(L_{11})_0$, and $(L_{22})_0$ at any constant z_1 all increase with increasing $\langle\bar{C}_T\rangle$. In addition, at any constant value of $\langle\bar{C}_T\rangle$, the values of $(L_{11})_V$ and $(L_{11})_0$ are largest as $z_1 \rightarrow 1$, whereas those of $(L_{22})_V$ and $(L_{22})_0$ are smallest. Correspondingly, the values of $(L_{22})_V$ and $(L_{22})_0$ are largest as $z_1 \rightarrow 0$, whereas those of $(L_{11})_V$ and $(L_{11})_0$ are smallest. That is, the values of $(L_{11})_V$, $(L_{22})_V$, $(L_{11})_0$, and $(L_{22})_0$ are largest when the composition fraction of the other component is smallest (i.e., as the composition approaches the binary solution of the major component) and decrease as the composition fraction of the other component increases (i.e., as the composition approaches the trace concentration in the binary solution of the other component). In general, at constant values of $\langle\bar{C}_T\rangle$, $(L_{11})_V$ is much greater than $(L_{22})_V$ and $(L_{11})_0$ is much greater than $(L_{22})_0$, but, surprisingly, when $z_1 = 0.25$, $(L_{11})_V \approx (L_{22})_V$ and $(L_{11})_0 \approx (L_{22})_0$.

Values of the cross-term diffusion Onsager coefficients $(L_{12})_V$, $(L_{21})_V$, $(L_{12})_0$, and $(L_{21})_0$ at constant z_1 all become increasingly more negative with increasing $\langle\bar{C}_T\rangle$. Curiously, these cross-term quantities as a function of z_1 at constant $\langle\bar{C}_T\rangle = (0.5, 1.0, \text{or } 1.5)$ mol·dm^{-3} all exhibit minima at $z_1 \approx 0.5$, i.e., when the chloride and sulfate concentrations are equal. However, many additional diffusion coefficient measurements at other values of z_1 near 0.5 would be needed to determine whether this

minimum always occurs at the same composition fraction or whether it varies slightly with $\langle \bar{C}_T \rangle$.

We now focus our attention on the solvent-fixed $(L_{ij})_0$ because they are the most useful for the theory of electrolyte solutions.

In addition to our experimental values at finite concentrations, we also include their values at infinite dilution in terms of expressions of the Nernst−Hartley type. The equations are in terms of equivalent conductances of the ions Λ_i^0 and salt Λ^0, and the equivalent fractions x_i, where $N = C_1 + 2C_2$, $x_1 = C_1/(C_1 + 2C_2)$, and $x_2 = 2C_2/(C_1 + 2C_2)$. At infinite dilution, these diffusion Onsager coefficient values are independent of the reference frame. The Nernst−Hartley expressions,[7] rewritten for the common cation case, are

$$\frac{(L_{11})_0}{x_1 N} = \frac{\Lambda_1^0[\Lambda^0 - x_1\Lambda_1^0]}{10^3(\nu_{1a}z_{1a})^2F^2\Lambda^0} \tag{29a}$$

$$\frac{(L_{22})_0}{x_2 N} = \frac{\Lambda_2^0[\Lambda^0 - x_2\Lambda_2^0]}{10^3(\nu_{2a}z_{2a})^2F^2\Lambda^0} \tag{29b}$$

$$\frac{(L_{12})_0}{x_1 x_2 N} = -\frac{\Lambda_1^0\Lambda_2^0}{10^3\nu_{1a}\nu_{2a}z_{1a}z_{2a}F^2\Lambda^0} \tag{29c}$$

$$\Lambda^0 = x_1\Lambda_1^0 + x_2\Lambda_2^0 + \Lambda_3^0 \tag{30}$$

where ν_{ia} is the stoichiometric coefficient of anion i; z_{ia} is the signed valence of anion i; F is Faraday's constant; and Λ_1^0, Λ_2^0, and Λ_3^0 are respectively the equivalent conductances of the Cl^- and SO_4^{2-} anions and the Na^+ common cation. Equations 29a−29c have most of the equivalent-fraction dependence removed, so they show less curvature than L_{ij} or L_{ij}/N. However, some curvature must remain when plotted against x_1 because x_i appears explicitly in the numerator of $(L_{ii})_0$ and because x_1 and $x_2 = 1 - x_1$ appear implicitly in the Λ^0 terms.

These infinite dilution values are contained in Table 10 at the z_1 molarity fraction corresponding to those of our experiments. The Λ_i^0 values used are taken from Robinson and Stokes[1] and whose values (after conversion from international to absolute ohms) are (76.312, 79.980, and 50.075) $\Omega^{-1}\cdot cm^2\cdot equiv^{-1}$ (where "equiv" denotes equivalent) respectively for Λ_1^0, Λ_2^0, and Λ_3^0.

There are several ways to plot our data, which include $(L_{ij})_0$, $(L_{ij})_0/N$, or $(L_{ii})_0/x_iN$ and $(L_{ij})_0/x_ix_jN$ (where $i \neq j$) plotted against x_i or $\langle \bar{C}_T \rangle$. As noted above, the latter two quantities should have less curvature.

Equations 29a−29c suggest that plotting $(L_{ii})_0/x_iN$ and $(L_{ij})_0/x_ix_jN$ against x_1 at various $\langle \bar{C}_T \rangle$ may minimize the curvature even at the higher $\langle \bar{C}_T \rangle$ concentrations. As suggested by eq 29c, the plots of $(L_{ij})_0/x_ix_jN$ should be "flatter" than the others, and it is found to be true. These plots against x_1 are shown in Figures 2−4. There is a curious crossover with $(L_{22})_0/x_2N$ plotted against x_1 for the infinite dilution and $\langle \bar{C}_T \rangle = 0.5$ mol·dm^{-3} curves. Furthermore, plots of $(L_{ij})_0$ and $(L_{ij})_0/N$ against x_1 all show minima for all values of $\langle \bar{C}_T \rangle$.

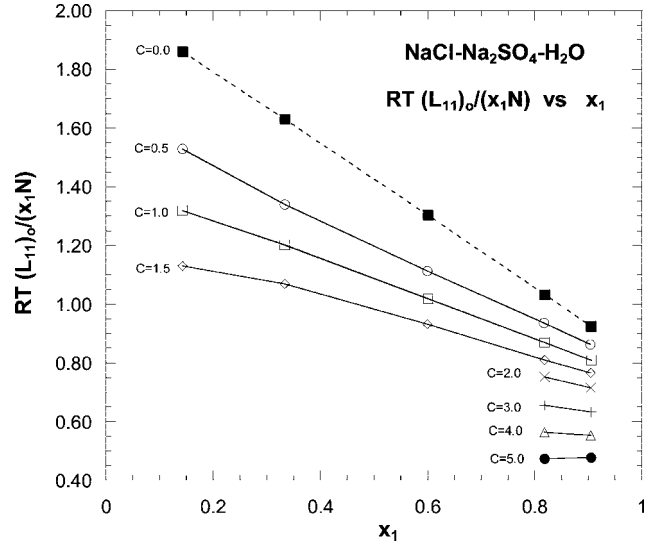

Figure 2. Values of $\{10^9\cdot RT(L_{11})_0/x_1N\}$/mol·equiv^{-1}·m^2·s^{-1} against x_1 at constant total molarity $\langle \bar{C}_T \rangle$/mol·dm^{-3}, where N is the total equivalent concentration of the electrolyte mixture and x_1 is the equivalent fraction of NaCl in the mixture [$N = C_1 + 2C_2$; $x_1 = C_1/(C_1 + 2C_2)$].

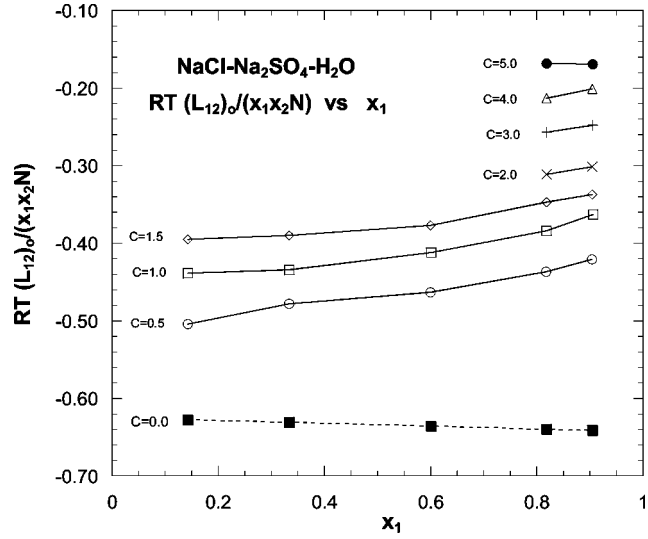

Figure 3. Values of $\{10^9\cdot RT(L_{12})_0/x_1x_2N\}$/mol·equiv^{-1}·m^2·s^{-1} against x_1 at constant total molarity $\langle \bar{C}_T \rangle$/mol·dm^{-3}, where N is the total equivalent concentration of the electrolyte mixture, x_1 is the equivalent fraction of NaCl, and x_2 is the equivalent fraction of Na_2SO_4 in the mixture [$N = C_1 + 2C_2$; $x_1 = C_1/(C_1 + 2C_2)$; $x_2 = 2C_2/(C_1 + 2C_2)$].

Plots of $(L_{ii})_0/x_iN$ and $(L_{ij})_0/x_ix_jN$ where $i \neq j$ plotted against $\langle \bar{C}_T \rangle$ at various values of x_1 show much more curvature than in Figures 2 to 4, as can be seen in Figures 5−7. The plots of $(L_{11})_0/x_1N$ against $\langle \bar{C}_T \rangle$ at any fixed value of x_1 (equivalent to plots at constant z_1) all decrease with increasing $\langle \bar{C}_T \rangle$ and with increasing x_1. The $(L_{11})_0/x_1N$ curves become steeper as the composition fraction of NaCl decreases. These curves at

Table 10. Nernst−Hartley Values of $RT(L_{11})_0/x_1N$, $RT(L_{22})_0/x_2N$, and $RT(L_{12})_0/x_1x_2N$ at Infinite Dilution and $T = 298.15$ K[a]

$10^9RT(L_{11})_0/x_1N$ / mol·equiv^{-1}·m^2·s^{-1}	$10^9RT(L_{22})_0/x_2N$ / mol·equiv^{-1}·m^2·s^{-1}	$10^9RT(L_{12})_0/x_1x_2N$ / mol·equiv^{-1}·m^2·s^{-1}	z_1	x_1
0.925 05	0.500 44	−0.641 21	0.95	0.904 76
1.033 50	0.471 51	−0.639 60	0.90	0.818 18
1.304 40	0.399 22	−0.635 60	0.75	0.600 00
1.630 90	0.312 08	−0.630 78	0.50	0.333 33
1.861 10	0.250 65	−0.627 37	0.25	0.142 86

[a] These are the limiting values of the diffusion Onsager coefficients when C_1 and C_2 vanish at molar ratios corresponding to z_1.

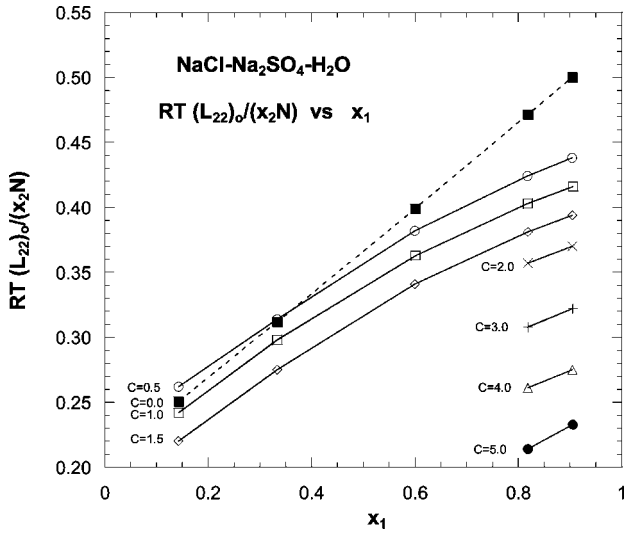

Figure 4. Values of $\{10^9 \cdot RT(L_{22})_0/x_2N\}$/mol·equiv^{-1}·m^2·s^{-1} against x_1 at constant total molarity $\langle \bar{C}_T \rangle$/mol·dm^{-3}, where N is the total equivalent concentration of the electrolyte mixture, x_1 is the equivalent fraction of NaCl, and x_2 is the equivalent fraction of Na_2SO_4 in the mixture [$N = C_1 + 2C_2$; $x_1 = C_1/(C_1 + 2C_2)$; $x_2 = 2C_2/(C_1 + 2C_2)$]. Note the crossover of the infinite dilution and $\langle \bar{C}_T \rangle = 0.5$ mol·dm^{-3} curves.

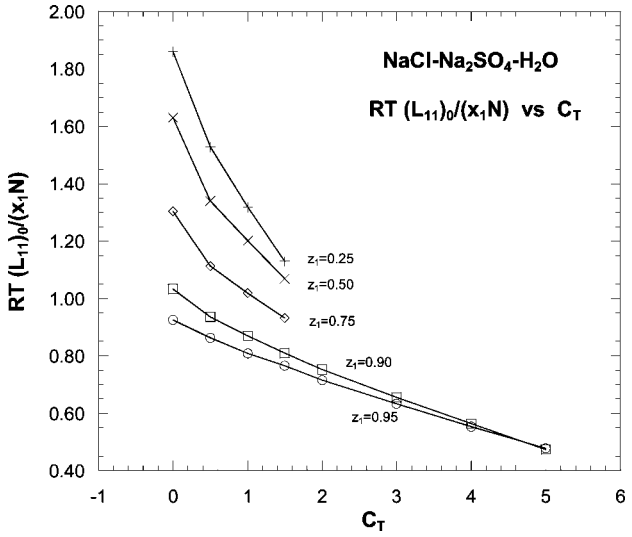

Figure 5. Values of $\{10^9 \cdot RT(L_{11})_0/x_1N\}$/mol·equiv^{-1}·m^2·s^{-1} against $\langle \bar{C}_T \rangle$/mol·dm^{-3} at constant molarity fraction z_1, where N is the total equivalent concentration of the electrolyte mixture and x_1 is the equivalent fraction of NaCl in the mixture [$N = C_1 + 2C_2$; $x_1 = C_1/(C_1 + 2C_2)$]. The points at each fixed value of z_1 were connected by straight lines.

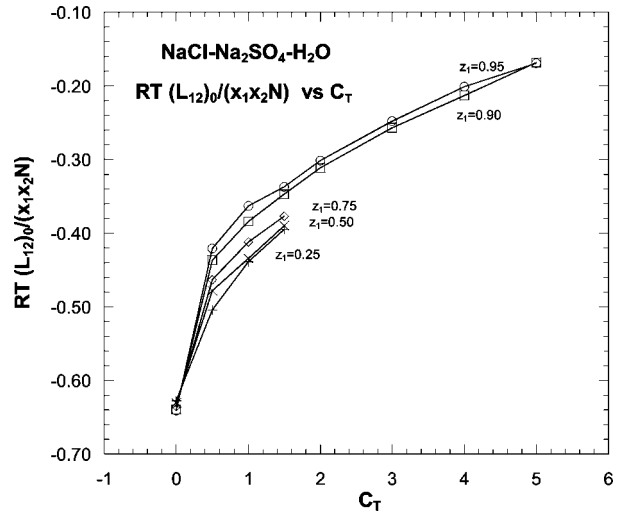

Figure 6. Values of $\{10^9 \cdot RT(L_{12})_0/x_1x_2N\}$/mol·equiv^{-1}·m^2·s^{-1} against $\langle \bar{C}_T \rangle$/mol·dm^{-3} at constant molarity fraction z_1, where N is the total equivalent concentration of the electrolyte mixture, x_1 is the equivalent fraction of NaCl, and x_2 is the equivalent fraction of Na_2SO_4 in the mixture [$N = C_1 + 2C_2$; $x_1 = C_1/(C_1 + 2C_2)$; $x_2 = 2C_2/(C_1 + 2C_2)$]. The points at each fixed value of z_1 were connected by straight lines.

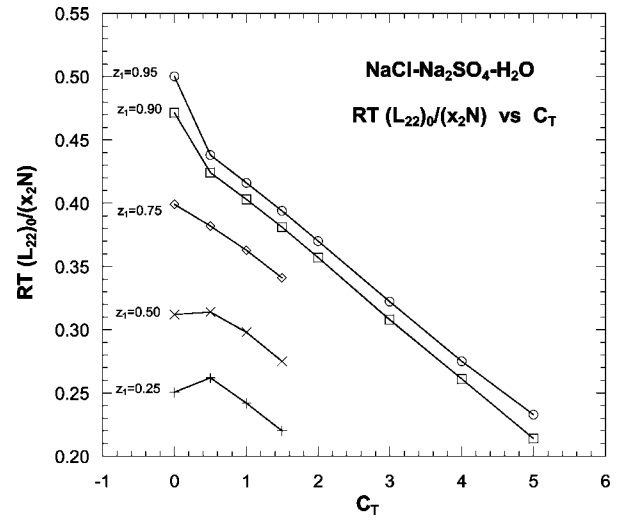

Figure 7. Values of $\{10^9 \cdot RT(L_{22})_0/x_2N\}$/mol·equiv^{-1}·m^2·s^{-1} against $\langle \bar{C}_T \rangle$/mol·dm^{-3} at constant molarity fraction z_1, where N is the total equivalent concentration of the electrolyte mixture and x_2 is the equivalent fraction of Na_2SO_4 in the mixture [$N = C_1 + 2C_2$; $x_1 = C_1/(C_1 + 2C_2)$; $x_2 = 2C_2/(C_1 + 2C_2)$]. The points at each fixed value of z_1 were connected by straight lines.

$x_1 = 0.90476$ and $x_1 = 0.81818$ ($z_1 = 0.95$ and $z_1 = 0.90$) converge at about $\langle \bar{C}_T \rangle = 5$ mol·dm^{-3}; the curves at lower values of x_1 also appear to be headed to this overlap point, but the measurements could not be made because of solubility limitations for Na_2SO_4 in the mixtures.

The corresponding plots of $(L_{12})_0/x_1x_2N$ against $\langle \bar{C}_T \rangle$ at various values of x_1 all increase with $\langle \bar{C}_T \rangle$ and x_1, i.e., become less negative. The increase with $\langle \bar{C}_T \rangle$ is especially steep between $\langle \bar{C}_T \rangle = (0$ and $0.5)$ mol·dm^{-3}, where there are no measurements to characterize the slopes. A few crossovers are apparent on these curves, but because of their small size, their significance is not clear. The negative values of this quantity were expected from the Nernst−Hartley infinite dilution values (Table 10).

The plots of $(L_{22})_0/x_2N$ against $\langle \bar{C}_T \rangle$ at any fixed value of x_1 (equivalent to plots at constant z_1) all decrease with increasing $\langle \bar{C}_T \rangle$ but increase with increasing x_1. Between $\langle \bar{C}_T \rangle = (0$ and $0.5)$ mol·dm^{-3}, where there are no measurements, the curves rise and then decrease (have a maximum) at $x_1 = 0.14286$ and $x_1 = 0.33333$ and show a regular decrease with increasing $\langle \bar{C}_T \rangle$ when $x_1 = 0.60$, with a reversal in the slope at higher values of x_1. The changes in the slope are not unexpected given that Na_2SO_4 is partially associated as $NaHSO_4^-$(aq), whereas Na^+ and Cl^- show little tendency to associate, but why the reversal in the initial slope occurs when $x_1 = 0.6$ ($z_1 = 0.75$) is not clear.

Plots of $(L_{ij})_0$ against x_1 and $(L_{ij})_0$ against $\langle \bar{C}_T \rangle$ (not shown) may be suitable for interpolation, despite their curvature and minima. Note that all values of $(L_{ij})_0$ are 0 at $\langle \bar{C}_T \rangle = 0$ for all x_1.

Test of the ORR Compared to Estimated Experimental Uncertainties

A direct comparison of $RT(L_{12})_V$ with $RT(L_{21})_V$ and of $RT(L_{12})_0$ with $RT(L_{21})_0$ provides a measure of the validity of the ORR. To the three significant figures reported in Table 7, in three cases $RT(L_{12})_V = RT(L_{21})_V$; in some other cases $RT(L_{12})_V$ is less negative than $RT(L_{21})_V$, but in other cases it is more negative. Similarly, for the solvent-fixed reference frame in Table 8, in four cases $RT(L_{12})_0 = RT(L_{21})_0$; in some other cases $RT(L_{12})_0$ is less negative than $RT(L_{21})_0$, but in other cases it is more negative. The values of the differences between $RT(L_{12})_R$ and $RT(L_{21})_R$ are generally small in both reference frames and show no obvious significant systematic variations with concentration.

As seen in Tables 7 and 8, the values of $RT(L_{12})_V$, $RT(L_{21})_V$, $RT(L_{12})_0$, and $RT(L_{21})_0$ vary by a factor of 10 from $-0.02 \cdot 10^{-12}$ to $-0.2 \cdot 10^{-12}$ mol·m^{-1}·s^{-1} as the total concentration and composition fraction are changed. The differences between $RT(L_{12})_V$ and $RT(L_{21})_V$ and between $RT(L_{12})_0$ and $RT(L_{21})_0$ at the same composition are generally small, $\leq 0.003 \cdot 10^{-12}$ mol·m^{-1}·s^{-1}, in all but four cases for each reference frame. The other four cases with slightly larger deviations tend to occur at higher concentrations.

As noted above, a more sensitive and quantitative test of the ORR (in which the quantities being compared only vary by a factor of 3) can be made by using the RHS and LHS of eq 28 for the volume-fixed reference frame, which we denote as LHS $= \{a_{11}(D_{12})_V + a_{12}(D_{22})_V\}/RT$ and RHS $= \{a_{21}(D_{11})_V + a_{22}(D_{21})_V\}/RT$.

Table 9 summarizes the values of the LHS and RHS of eq 28, their difference LHS − RHS (with sign), and the uncertainty of this difference calculated from the uncertainties of the input quantities using the propagation-of-errors method. At 8 compositions, the differences are small and positive, and at the other 15 compositions, they are small and negative. In 18 cases, the differences are well within the calculated uncertainties, thus indicating that the ORR is obeyed well within experimental error. In four other cases, the differences are slightly larger but still adequately within the assigned experimental error. At the only other compositions, $\langle \bar{C}_1 \rangle = 2.700\,25$ mol·dm^{-3} and $\langle \bar{C}_2 \rangle = 0.300\,04$ mol·dm^{-3}, the difference is $0.014 \cdot 10^{-12}$ m^5·mol^{-1}·s^{-1}, which only slightly exceeds the calculated uncertainty of $0.012 \cdot 10^{-12}$ m^5·mol^{-1}·s^{-1}. Given that the ORR for ternary-solution isothermal diffusion is obeyed within experimental uncertainty at 22 of 23 compositions, the small discrepancy at the other composition is likely just due to a slight underestimation of the experimental uncertainty of one or more of the diffusion coefficients.

Summary

We used previously reported[17−21] precise diffusion and density measurements for the NaCl + Na_2SO_4 + H_2O system at 298.15 K at 23 overall compositions spanning a wide composition range to test the ORR for isothermal diffusion. Realistic errors were assigned to the individual diffusion coefficients from cross-plotting and an earlier "rule-of-thumb" based on subset analysis for diffusion measurements at the same overall composition.[11,36] Available isopiestic data[24,33] for this system were reanalyzed with a hybrid thermodynamic model that was then used to calculate the chemical-potential concentration derivatives and estimate their uncertainties. These results were combined to calculate the diffusion Onsager coefficients on both the volume-fixed and solvent-fixed reference frames, $(L_{ij})_V$ and $(L_{ij})_0$, respectively. The ORR for ternary-solution diffusion was found to be obeyed within the assigned uncertainty limits at 22 of 23 compositions, and the very minor discrepancy at the other composition is probably due to a slight underestimation of the uncertainties for the diffusion coefficients. These results give very extensive and rigorous tests, and possibly the most accurate test, of the ORR for ternary-solution diffusion.

Appendix

We briefly describe the relations between various descriptions of the D_{ij} and L_{ij}, their transformations, and equations needed for the ORR tests. These are obtained most transparently using the matrix methods described by De Groot and Mazur.[37] We use the following notation taken from a comprehensive summary of previous work (containing the original references) showing how irreversible thermodynamics leads to the complete macroscopic description of liquid-state diffusion.[4]

For an arbitrary reference frame R

$$\mathbf{J}^R = \mathbf{D}^R \mathbf{C} \tag{A1}$$

$$\mathbf{J}^R = \mathbf{L}^R \mathbf{Y}^R \tag{A2}$$

where $\mathbf{J}^R$, $\mathbf{C}$, and $\mathbf{Y}^R$ are the respective column vectors of the flows, negative concentration gradients, and driving forces of irreversible thermodynamics for reference frame R and where $\mathbf{D}^R$ and $\mathbf{L}^R$ are the respective square matrices of the diffusion coefficients and diffusion Onsager coefficients. Transformation of $\mathbf{J}^R$, $\mathbf{L}^R$, and $\mathbf{Y}^R$ between different reference frames requires that the "entropy production" of irreversible thermodynamics be invariant.[4,37]

The elements of the negative concentration gradient matrix $\mathbf{C}$ are

$$C_i' = -\partial C_i/\partial x \tag{A3}$$

The simplest $\mathbf{Y}^R$ is that for the solvent-fixed reference frame, $\mathbf{Y}^0 = \mathbf{X}$, whose elements are

$$X_i = (\partial G_i/\partial x)_{p,T} \tag{A4}$$

The elements X_i of the $\mathbf{X}$ matrix can be written as

$$X_i = \sum_k \left(\frac{\partial G_i}{\partial C_k}\right)\left(-\frac{\partial C_k}{\partial x}\right) \tag{A5}$$

or

$$\mathbf{X} = \boldsymbol{\mu}\mathbf{C} \tag{A6}$$

and where the elements of $\boldsymbol{\mu}$ are

$$\mu_{ik} = \frac{\partial G_i}{\partial C_k} \tag{A7}$$

Solvent-Fixed Reference Frame.

For this reference frame,

$$\mathbf{J}^0 = \mathbf{D}^0\mathbf{C} = \mathbf{L}^0\mathbf{X} = \mathbf{L}^0\boldsymbol{\mu}\mathbf{C} \tag{A8}$$

from which

$$\mathbf{D}^0 = \mathbf{L}^0\boldsymbol{\mu} \tag{A9}$$

and

$$\mathbf{L}^0 = \mathbf{D}^0\boldsymbol{\mu}^{-1} \tag{A10}$$

The individual $(L_{ij})_0$ are our desired diffusion Onsager coefficients and are given explicitly by eqs 23a to 23d.

Unfortunately, for more than three components, the expressions for $\boldsymbol{\mu}^{-1}$ contain increasingly complicated terms involving products of $(n-2)\mu_{ij}$ terms divided by the product of $(n-$

1)μ_{ij} terms. Consequently, the calculations of the $(L_{ij})_0$ terms are even more complicated.

Volume-Fixed Reference Frame.

For this reference frame,

$$\mathbf{J}^V = \mathbf{D}^V\mathbf{C} = \mathbf{L}^V\mathbf{Y}^V \tag{A11}$$

However, it has been shown[4] that

$$\mathbf{Y}^V = \tilde{A}^{0V}\mathbf{X} = \tilde{A}^{0V}\boldsymbol{\mu}\mathbf{C} \tag{A12}$$

where the tilde represents the transpose of a matrix. Thus, the elements of $\tilde{\mathbf{A}}^{0V}$ are

$$\tilde{A}_{ij}^{0V} = \alpha_{ij} = A_{ji}^{0V} \tag{A13}$$

and where[4]

$$A_{ij}^{0V} = \delta_{ij} + \frac{C_i\bar{V}_j}{C_0\bar{V}_0} \tag{A14}$$

Consequently,

$$\mathbf{D}^V = \mathbf{L}^V\tilde{A}^{0V}\boldsymbol{\mu} \tag{A15}$$

and

$$\mathbf{L}^V = \mathbf{D}^V\boldsymbol{\mu}^{-1}(\tilde{A}^{0V})^{-1} \tag{A16}$$

The four $(L_{ij})^V$ components of $\mathbf{L}^V$ are given explicitly in eqs 25a to 25d.[10,14] We note that from the definition[4] of A_{ij}^{RS}

$$(A_{ij}^{0V})^{-1} = A_{ij}^{V0} = \delta_{ij} - \frac{C_i\bar{V}_j}{10^3} \tag{A17}$$

which is ϵ_{ji} of ref 14 (note the reversed subscript of ϵ_{ij}).

Again, unfortunately, for more than three components, the expressions for $\boldsymbol{\mu}^{-1}$ contain increasingly complicated terms involving the products of μ_{ij}. Consequently, the calculations of the $(L_{ij})_V$ terms are also more complicated.

Other Matrix Results.

It can be shown[4] that

$$\mathbf{D}^0 = \mathbf{A}^{0V}\mathbf{D}^V \tag{A18}$$

whose component form was given in eq 20, which allows $(D_{ij})_0$ to be calculated from the experimental $(D_{ij})_V$.

Furthermore, the relationship of $\boldsymbol{\mu}$ and $\boldsymbol{\mu}^m$ is

$$\boldsymbol{\mu} = \left(\frac{1}{C_0M_0}\right)\boldsymbol{\mu}^m\mathbf{A}^{0V} \tag{A19}$$

where, as noted earlier, the elements $\mu_{ij}^m = (\partial G_i/\partial m_j)_{p,T}$ of $\boldsymbol{\mu}^m$ are related to the activity coefficient derivatives by eqs 14a and 14b.

Transformed Test of the ORR.

The matrix form of the ORR is

$$\mathbf{L}^R = \tilde{\mathbf{L}}^R \tag{A20}$$

or $L_{ij}^R = L_{ji}^R$. The simplest example is the solvent-fixed case, where from eqs A10 and A20

$$\mathbf{L}^0 = \mathbf{D}^0\boldsymbol{\mu}^{-1} = \tilde{\boldsymbol{L}}^0 = \tilde{\boldsymbol{\mu}}^{-1}\tilde{\boldsymbol{D}}^0 \tag{A21}$$

If we multiply both sides of this equation on the left by $\tilde{\boldsymbol{\mu}}$ and on the right by $\boldsymbol{\mu}$, we get the equivalent equation

$$\tilde{\boldsymbol{\mu}}\mathbf{D}^0 = \tilde{\boldsymbol{D}}^0\boldsymbol{\mu} \tag{A22}$$

whose component form is

$$\sum_{k=1}^{n}\mu_{ki}D_{kj}^0 = \sum_{k=1}^{n}D_{ki}^0\mu_{kj} \tag{A23}$$

This gives n equations for $i = j$, whose results are identities. For $i \neq j$, there are $(n^2 - n)/2$ nontrivial equations equivalent to the ORR but which have the great advantage that they are *linear in* μ_{ij} for any number of components, unlike the direct comparison of the L_{ij}^0 expressions themselves.

This result for the ternary-solution solvent-fixed case was first given by Onsager[3] and generalized by Hooyman and De Groot as described by De Groot and Mazur.[37]

As mentioned earlier, it is advantageous to work directly with the experimental D_{ij}^V to minimize the estimated errors, i.e., within the volume-fixed reference frame. Thus, using eq A16 for $\mathbf{L}^V$, the ORR are

$$\mathbf{L}^V = \mathbf{D}^V\boldsymbol{\mu}^{-1}(\tilde{\boldsymbol{A}}^{0V})^{-1} = \tilde{\boldsymbol{L}}^V = (\mathbf{A}^{0V})^{-1}\tilde{\boldsymbol{\mu}}^{-1}\tilde{\mathbf{D}}^V \tag{A24}$$

By multiplying on the left by $\mathbf{A}^{0V}$ and then by $\tilde{\boldsymbol{\mu}}$ and on the right by $\tilde{\mathbf{A}}^{0V}$ and then $\boldsymbol{\mu}$, we get

$$\tilde{\boldsymbol{\mu}}\mathbf{A}^{0V}\mathbf{D}^V = \tilde{\mathbf{D}}^V\tilde{\mathbf{A}}^{0V}\boldsymbol{\mu} \tag{A25}$$

The resulting expressions are *linear in* μ_{ij} for any number of components, unlike the L_{ij} expressions themselves.

The component form of eq A25 is

$$\sum_k\sum_l\mu_{ki}A_{kl}^{0V}(D_{lj})_V = \sum_k\sum_l(D_{ki})_VA_{lk}^{0V}\mu_{lj} \tag{A26}$$

There is one nontrivial ORR for a three-component system, three for a four-component one, and six for a five-component one. As noted earlier, the matrix of α_{ij} equals the matrix $\tilde{\mathbf{A}}^{0V}$, whose components are A_{ji}^{0V} (note the reversed indices). Equation 28 follows from the above result.

Acknowledgment

We congratulate and dedicate this paper to Professor Robin Stokes on the occasion of his 90th birthday. His book (with R. A. Robinson) *Electrolyte Solutions* remains a constant reference source for our work, and in most areas of our research, Prof. Stokes has published significant pioneering research.

Literature Cited

(1) Robinson, R. A.; Stokes, R. H. *Electrolyte Solutions*, 2nd ed. (Revised); Butterworth: London, 1965.
(2) Onsager, L.; Fuoss, R. M. Irreversible Processes in Electrolytes. Diffusion, Conductance, and Viscous Flow in Arbitrary Mixtures of Strong Electrolytes. *J. Phys. Chem.* **1932**, *36*, 2689–2778.
(3) Onsager, L. Theories and Problems of Liquid Diffusion. *Ann. N.Y. Acad. Sci.* **1945**, *46*, 241–265.
(4) Miller, D. G.; Vitagliano, V.; Sartorio, R. Some Comments on Multicomponent Diffusion: Negative Main Term Diffusion Coefficients, Second Law Constraints, and Reference Frame Transformations. *J. Phys. Chem.* **1986**, *90*, 1509–1519.
(5) Kirkwood, J. G.; Baldwin, R. L.; Dunlop, P. J.; Gosting, L. J.; Kegeles, G. Flow Equations and Frames of Reference for Isothermal Diffusion in Liquids. *J. Chem. Phys.* **1960**, *33*, 1505–1513.
(6) Miller, D. G. Application of Irreversible Thermodynamics to Electrolyte Solutions. I. Determination of Ionic Transport Coefficients l_{ij} for Isothermal Vector Transport Processes in Binary Electrolyte Systems. *J. Phys. Chem.* **1966**, *70*, 2639–2659.
(7) Miller, D. G. Application of Irreversible Thermodynamics to Electrolyte Solutions. II. Ionic Coefficients l_{ij} for Isothermal Vector Transport Processes in Ternary Systems. *J. Phys. Chem.* **1967**, *71*, 616–632.
(8) Miller, D. G. Application of Irreversible Thermodynamics to Electrolyte Solutions. III. Equations for Isothermal Vector Transport Processes in *n*-Component Systems. *J. Phys. Chem.* **1967**, *71*, 3588–3592.
(9) Vitagliano, V.; Costantino, L.; D'Errico, G.; Ortona, O.; Paduano, L.; Sartorio, R.; Vergara, A.; Miller, D. G.; Albright, J. G.; Annunziata, O. The History of Interferometry for Measuring Diffusion Coefficients. The Contribution of Neapolitan Group to the Studies of Mutual Diffusion. *Rend. Accad. Sci. Fis. Mat., Naples* **2007**, *LXXIV*, 191–268.

(10) Miller, D. G. Ternary Isothermal Diffusion and the Validity of the Onsager Reciprocity Relations. *J. Phys. Chem.* **1959**, *63*, 570–578.
(11) Miller, D. G.; Albright, J. G.; Mathew, R.; Lee, C. M.; Rard, J. A.; Eppstein, L. B. Isothermal Diffusion Coefficients of $NaCl-MgCl_2-H_2O$ at 25 °C. 5. Solute Concentration Ratio of 1:1 and Some Rayleigh Results. *J. Phys. Chem.* **1993**, *97*, 3885–3899.
(12) Rard, J. A.; Miller, D. G. Ternary Mutual Diffusion Coefficients of $ZnCl_2-KCl-H_2O$ at 25 °C by Rayleigh Interferometry. *J. Solution Chem.* **1990**, *19*, 129–148.
(13) Miller, D. G. Thermodynamics of Irreversible Processes. The Experimental Verification of the Onsager Reciprocal Relations. *Chem. Rev.* **1960**, *60*, 15–37.
(14) Woolf, L. A.; Miller, D. G.; Gosting, L. J. Isothermal Diffusion Measurements on the System H_2O-Glycine$-$KCl at 25°; Tests of the Onsager Reciprocal Relation. *J. Am. Chem. Soc.* **1962**, *84*, 317–331.
(15) Leaist, D. G.; Lyons, P. A. Multicomponent Diffusion in Dilute Solutions of Mixed Electrolytes. *Aust. J. Chem.* **1980**, *33*, 1869–1887.
(16) Gosting, L. J.; Kim, H.; Loewenstein, M. A.; Reinfelds, G.; Revzin, A. A Versatile Optical Diffusiometer Including a Large Optical Bench of New Design. *Rev. Sci. Instrum.* **1973**, *44*, 1602–1609.
(17) Rard, J. A.; Albright, J. G.; Miller, D. G.; Zeidler, M. E. Ternary Mutual Diffusion Coefficients and Densities of the System $\{z_1$NaCl $+ (1- z_1)Na_2SO_4\}$(aq) at 298.15 K and a Total Molarity of 0.5000 mol dm^{-3}. *J. Chem. Soc., Faraday Trans.* **1996**, *92*, 4187–4197.
(18) Albright, J. G.; Gillespie, S. M.; Rard, J. A.; Miller, D. G. Ternary Solution Mutual Diffusion Coefficients and Densities of Aqueous Mixtures of NaCl and Na_2SO_4 at 298.15 K for Six Different Solute Fractions at a Total Molarity of 1.000 mol·dm^{-3}. *J. Chem. Eng. Data* **1998**, *43*, 668–675.
(19) Annunziata, O.; Rard, J. A.; Albright, J. G.; Paduano, L.; Miller, D. G. Mutual Diffusion Coefficients and Densities at 298.15 K of Aqueous Mixtures of NaCl and Na_2SO_4 for Six Different Solute Fractions at a Total Molarity of 1.500 mol·dm^{-3} and of Aqueous Na_2SO_4. *J. Chem. Eng. Data* **2000**, *45*, 936–945.
(20) Fu, J.; Paduano, L.; Rard, J. A.; Albright, J. G.; Miller, D. G. Mutual Diffusion Coefficients and Densities at 298.15 K of Aqueous Mixtures of NaCl and Na_2SO_4 at High Concentrations with NaCl Solute Fractions of 0.9000. *J. Chem. Eng. Data* **2001**, *46*, 601–608.
(21) Fu, J.; Rard, J. A.; Paduano, L.; Albright, J. G.; Miller, D. G. Mutual Diffusion Coefficients and Densities at 298.15 K of Aqueous Mixtures of NaCl and Na_2SO_4 with NaCl Solute Fractions of 0.9500, Trace Diffusion Coefficients of SO_4^{2-} in NaCl(aq), and Trace Refractive Index Increments and Partial Molar Volumes of Na_2SO_4 and NaCl. *J. Chem. Eng. Data* **2002**, *47*, 496–512.
(22) Rard, J. A.; Miller, D. G. The Mutual Diffusion Coefficients of $NaCl-H_2O$ and $CaCl_2-H_2O$ at 25 °C from Rayleigh Interferometry. *J. Solution Chem.* **1979**, *8*, 701–716.
(23) Rard, J. A.; Miller, D. G. The Mutual Diffusion Coefficients of $Na_2SO_4-H_2O$ and $MgSO_4-H_2O$ at 25 °C from Rayleigh Interferometry. *J. Solution Chem.* **1979**, *8*, 755–766.
(24) Rard, J. A.; Clegg, S. L.; Platford, R. F. Thermodynamics of $\{z$NaCl $+ (1- z)Na_2SO_4\}$(aq) from $T = 278.15$ K to $T = 313.15$ K, and Representation with an Extended Ion-Interaction (Pitzer) Model. *J. Chem. Thermodyn.* **2003**, *35*, 967–1008.
(25) Pitzer, K. S. Ion Interaction Approach: Theory and Data Correlation. In *Activity Coefficients in Electrolyte Solutions*, 2nd ed.; Pitzer, K. S., Ed.; CRC Press: Boca Raton, FL, 1991; Chapter 3.
(26) (a) Scatchard, G. Osmotic Coefficients and Activity Coefficients in Mixed Electrolyte Solutions. *J. Am. Chem. Soc.* **1961**, *83*, 2636–2642. (b) Corrections for this paper are given in footnote 6 of: Rush, R. M.; Johnson, J. S. Isopiestic Measurements of the Osmotic and Activity Coefficients for the Systems $HClO_4-LiClO_4-H_2O$, $HClO_4-NaClO_4-H_2O$, and $LiClO_4-NaClO_4-H_2O$. *J. Phys. Chem.* **1968**, *72*, 767–774.
(27) Miller, D. G. Activity Coefficient Derivatives of Ternary Systems Based on Scatchard's Neutral Electrolyte Description. *J. Solution Chem.* **2008**, *37*, 365–375.
(28) Pavićević, V.; Ninković, R.; Todorović, M.; Miladinović, J. Osmotic and Activity Coefficients of $\{y NaH_2PO_4 + (1- y)Na_2SO_4\}$(aq) at the Temperature 298.15 K. *Fluid Phase Equilib.* **1999**, *164*, 275–284.
(29) Miladinović, J.; Ninković, R.; Todorović, M.; Rard, J. A. Isopiestic Investigation of the Osmotic and Activity Coefficients of $\{y MgCl_2 + (1- y)MgSO_4\}$(aq) and the Osmotic Coefficients of $Na_2SO_4 \cdot MgSO_4$(aq) at 298.15 K. *J. Solution Chem.* **2008**, *37*, 307–329.
(30) Archer, D. G. Thermodynamic Properties of the $NaCl + H_2O$ System. II. Thermodynamic Properties of NaCl(aq), $NaCl \cdot 2H_2O$(cr), and Phase Equilibria. *J. Phys. Chem. Ref. Data* **1992**, *21*, 793–829.
(31) Archer, D. G.; Wang, P. The Dielectric Constant of Water and Debye–Hückel Limiting Law Slopes. *J. Phys. Chem. Ref. Data* **1990**, *19*, 371–411.
(32) Wu, Y. C.; Rush, R. M.; Scatchard, G. Osmotic and Activity Coefficients for Binary Mixtures of Sodium Chloride, Sodium Sulfate, Magnesium Sulfate, and Magnesium Chloride at 25°. I. Isopiestic Measurements on the Four Systems with Common Ions. *J. Phys. Chem.* **1968**, *72*, 4048–4053.
(33) Robinson, R. A.; Platford, R. F.; Childs, C. W. Thermodynamics of Aqueous Mixtures of Sodium Chloride, Potassium Chloride, Sodium Sulfate, and Potassium Sulfate at 25 °C. *J. Solution Chem.* **1972**, *1*, 167–172.
(34) Filippov, V. K.; Cheremnykh, L. M. Application of Pitzer's Method to the Solubility Calculations in the $Na||Cl,SO_4-H_2O$ and $K||Cl,SO_4-H_2O$ Systems at 25 °C. *Vestn. Leningr. Univ., Ser. Mat., Fiz. Khim.* **1986**, *1*, 46–50.
(35) Dunlop, P. J.; Gosting, L. J. Use of Diffusion and Thermodynamic Data to Test the Onsager Reciprocal Relation for Isothermal Diffusion in the System $NaCl-KCl-H_2O$ at 25°. *J. Phys. Chem.* **1959**, *63*, 86–93.
(36) Miller, D. G.; Paduano, L.; Sartorio, R.; Albright, J. G. Analysis of Gouy Fringe Data and Comparison of Rayleigh and Gouy Optical Diffusion Measurements Using the System Raffinose (0.015 M)$-$KCl (0.5 M)$-H_2O$ at 25 °C. *J. Phys. Chem.* **1994**, *98*, 13745–13754.
(37) De Groot, S. R.; Mazur, P. *Non-Equilibrium Thermodynamics*; North-Holland Publishing Co.: Amsterdam, The Netherlands, and Wiley Interscience: New York, 1962.

Received for review September 29, 2008. Accepted November 15, 2008.

JE800725K